Andreia Marisa da Silva Fortuna

Licenciada em Bioquímica

Gold nanoprobes for assessing expression of critical genes in the infection pathway of MRSA

Dissertação para obtenção do Grau de Mestre em Biotecnologia

Orientador: Prof. Doutora Rita Gonçalves Sobral, FCT/UNL
Co-orientador: Prof. Doutor Pedro Viana Baptista, FCT/UNL

Júri:

Presidente: Prof. Doutora Ana Cecília Afonso Roque
Arguente: Doutora Teresa Conceição
Vogal: Prof. Doutora Rita Gonçalves Sobral

FACULDADE DE CIÊNCIAS E TECNOLOGIA
UNIVERSIDADE NOVA DE LISBOA

[Setembro 2015]

Gold nanoprobes for assessing expression of critical genes in the infection pathway of MRSA

My master thesis allowed me to contribute to this following publication:

Larguinho, M., Canto, R., Cordeiro, M., Pedrosa, P., Fortuna, A., Vinhas, R., Baptista, P.V. 2015. Gold nanoprobe-based non-crosslinking hybridization for molecular diagnostics. Expert Rev Mol Diagn. 1-14.

Acknowledgments

I could not have performed this work without the help of several people and the support from the institution that contributed to its success. In this regard, I would like to thank all of those who in one way or another helped me whenever I needed during the course of this project.

First of all I would like to thank all the teachers that contributed to my academic path and the Institution, Faculdade de Ciências e Tecnologia da Universidade Nova de Lisboa, that provided me with the facilities and conditions, crucial for my learning process.

I want to express my gratitude to my supervisors, Prof. Rita Sobral and Prof. Pedro Viana Baptista: for all the opportunities they have given me; for having received me in their laboratories; for sharing knowledge; for scientific guidance and for calling me attention; for their patience and support.

I have to extend my gratitude to all my laboratory colleagues: Ana Bárbara Carreira, Ana Sofia Matias, Bárbara Gonçalves, Bruno Veigas, Fábio Carlos, Joana Silva, João Jesus, Letícia Giestas, Miguel Larguinho, Milton Cordeiro, Pedro Pedrosa, Rafaela Canto, Raquel Portela, Raquel Vinhas, Rita Cabral, Sara Figueiredo. I would like to thank you all: for the support, the advices and suggestions; for the availability, the encouragement and the guidance in the laboratory; for all the laughs and good moments.

A special acknowledgement to my colleagues and friends Ana Bárbara Carreira and Rafaela Canto: thank you for your unconditional support and strength given throughout this year.

To all my closest friends who have always supported and encouraged me, I am very grateful to them for being there whenever I needed them, for the advices given, the patience and for all the joys.

A special acknowledgement to Fernando Gonçalves for the motivation given and for believing in me.

Finally, I am immensely grateful to my family, specially my parents and brother for the love, unconditional support, comprehension, patience and for never doubting me.

Thank you all!

Resumo

Staphylococcus aureus é um agente patogénico oportunista clinicamente relevante responsável por uma enorme variedade de doenças, desde situações ligeiras até às que envolvem risco de vida. *S. aureus* pode colonizar diversas partes do corpo humano, sendo as fossas nasais anteriores o seu nicho ecológico primário. A sua importância clínica deve-se à sua habilidade de resistir a quase todas as classes de antibióticos disponíveis, associado a um elevado número de fatores de virulência. As estirpes de MRSA (Methicillin-Resistant *S. aureus*) são particularmente importantes no contexto hospitalar, sendo a maior causa mundial de infeções nosocomiais.

A resistência das estirpes MRSA aos antibióticos β-lactâmicos envolve a aquisição do gene *mecA*, incluído na cassete SCC*mec*.

Técnicas de diagnóstico rápidas e confiáveis são necessárias para a redução da mortalidade e morbilidade associadas às infeções por MRSA, através da identificação precoce do agente de infeção. As técnicas de identificação atuais normalmente demoram 5 dias para determinar o perfil de resistência aos antibióticos. Têm sido desenvolvidas diversas técnicas baseadas em amplificação de forma a acelerar o diagnóstico.

O nosso principal objetivo foi desenvolver uma metodologia ainda mais rápida que evitasse o passo de amplificação de DNA. Foram usadas nanossondas de ouro para detetar a presença do gene *mecA* no genoma de *S. aureus*, associado a padrões de resistência, para ensaios colorimétricos baseados no método de *non-crosslinking*.

Os nossos resultados mostraram que as nanossondas de ouro mecA e mecA_V2 são suficientemente sensíveis para discriminar a presença do gene *mecA* em produtos de PCR e em amostras de DNA genómico (gDNA) para concentrações de alvo de 10 ng/µL e 20 ng/µL, respetivamente. Como o nosso principal objetivo implicava a eliminação do passo de amplificação, concluímos que a melhor metodologia de identificação de MRSA num estado inicial de infeção é a realização de ensaios colorimétricos baseados no método de *non-crosslinking* com amostras de gDNA, que podem ser extraídas diretamente de amostras de sangue.

Palavras-chave: *Staphylococcus aureus*, resistência aos antibióticos β-lactâmicos, MRSA, gene *mecA*, nanopartículas de ouro, diagnóstico.

Abstract

Staphylococcus aureus is an important opportunistic pathogen that can cause a wide variety of diseases from mild to life-threatening conditions. *S. aureus* can colonize many parts of the human body but the anterior nares are the primary ecological niche. Its clinical importance is due to its ability to resist almost all classes of antibiotics available together with its large number of virulence factores. MRSA (Methicillin-Resistant *S. aureus*) strains are particularly important in the hospital settings, being the major cause of nosocomial infections worldwide.

MRSA resistance to β-lactam antibiotics involves the acquisition of the exogenous *mecA* gene, part of the SCC*mec* cassette.

Fast and reliable diagnostic techniques are needed to reduce the mortality and morbidity associated with MRSA infections, through the early identification of MRSA strains. The current identification techniques are time-consuming as they usually involves culturing steps, taking up to five days to determine the antibiotic resistance profile. Several amplification-based techniques have been developed to accelerate the diagnosis.

The aim of this project was to develop an even faster methodology that bypasses the DNA amplification step. Gold-nanoprobes were developed and used to detect the presence of *mecA* gene in *S. aureus* genome, associated with resistance traits, for colorimetric assays based on non-crosslinking method.

Our results showed that the mecA and mecA_V2 gold-nanoprobes were sensitive enough to discriminate the presence of *mecA* gene in PCR products and genomic DNA (gDNA) samples for target concentrations of 10 ng/µL and 20 ng/µL, respectively. As our main objective was to avoid the amplification step, we concluded that the best strategy for the early identification of MRSA infection relies on colorimetric assays based on non-crosslinking method with gDNA samples that can be extracted directly from blood samples.

Keywords: *Staphylococcus aureus*, resistance to β-lactams, MRSA, *mecA* gene, gold nanoparticles, diagnostics.

Table of contents

Figures Index

Tables Index

Abbreviations

Abs – Absorbance

AL – Alkaline Lysis

AUC – Area under the curve

AuNPs – Gold Nanoparticles

bp – base pair

CA-MRSA - Community-Associated Methicillin-resistant *Staphylococcus aureus*

DLS – Dynamic Light Scattering

DNA – Deoxyribonucleic Acid

dNTPs – Deoxyribonucleotide Triphosphate

DTT – Dithiothreitol

gDNA – genomic DNA

HA-MRSA - Health care-Associated Methicillin-resistant *Staphylococcus aureus*

LB – Luria Bertani

MRSA – Methicillin-resistant *Staphylococcus aureus*

MSSA – Methicillin-susceptible *Staphylococcus aureus*

NCL – Non-crosslinking

PBP – Penicillin Binding Protein

PCR – Polymerase Chain Reaction

pDNA – plasmid DNA

RNA – Ribonucleic Acid

SCC*mec* – Staphylococcal chromosome cassette *mec*

SDS – Sodium Dodecyl Sulfate

SPR – Surface Plasmon Resonance

TEM – Transmission Electronic Microscopy

TSA – Tryptic Soy Agar

TSB – Tryptic Soy Broth

UV-vis – Ultraviolet-visible spectroscopy

1. Introduction

1.1. Staphylococci

The genus *Staphylococcus* was introduced for the first time by Ogston in 1883 for the members of the micrococci group that have round-shaped cells, arrange as grape-like clusters, produce inflammation and suppuration develop violet coloration in the staining method (gram-positive bacteria). *Staphylococcus* genus includes over 40 different species, most of them animal commensals; the common phenotypic characteristics include being facultative anaerobes and catalase producers, capable to convert hydrogen peroxide to water and oxygen. Staphylococci are organized into two major groups, according to their capacity to produce coagulase, an enzyme that causes blood clot formation (Ogston, 1883).

1.2. *Staphylococcus aureus* – an important human pathogen

A high number of hospital infections is caused by a specific species of coagulase positive staphylococci, *Staphylococcus aureus* (Solberg, 1965), name attributed by Rosenbach (Rosenbach, 1884).

Staphylococcus aureus is a commensal bacteria that colonizes the skin of healthy people. It is also an important opportunistic pathogen that can cause a wide variety of diseases, from mild conditions, such as skin infections like cellulitis, folliculitis, impetigo, abscesses, to life-threatening situations, such as pneumonia, endocarditis, meningitis, or toxic-shock syndrome (Foster, 2005), depending on its intrinsic virulence or the ability of the host to contain its opportunistic behavior (Grundman *et al*., 2006). Also, due to its capacity to produce exotoxins as virulence factors, *S. aureus* can be responsible for food poisoning (Lee, 2003).

Besides the skin, *S. aureus* can colonize other parts of the human body, such as the respiratory and the genitourinary tract (Skinner *et al*., 1941). However, the nose, specifically the anterior nares, is the primary ecological niche (Vanderbergh and Verbrugh, 1996).

In the pre-antibiotic era, *S. aureus* infections were responsible for the death of more than 80% of the infected patients. Moreover, 70% of the patients developed metastatic infections. The common treatment were general supportive measures, blood transfusions to supply red and leukocytes cells, surgical drainage of loci of infection and the administration of antitoxins to neutralize the circulating toxins (Skinner *et al*., 1941).

With the implementation of antibiotics for the treatment of infections, *S. aureus* immediately emerged as a highly versatile pathogen, showing the capacity to develop resistance to most classes of antibiotics (multi-resistant strains) and to spread worldwide through a number of successful clonal lineages (Vanderbergh and Verbrugh, 1996).

S. aureus is an important human pathogen not only due to its capacity to resist antibiotics but also due to its virulence characteristics. In fact, *S. aureus* has many virulence factors that play different roles in the infective process, such as mediating the attachment to the host cells (fibrinogen-binding proteins or coagulase) (Foster *et al*., 1998), preventing the impact of host

defense mechanisms (biofilm forming elements or protein A) (Skaar *et al*., 2004) and allowing the invasion and tissue penetration (leukocidins and enterotoxins) (Dinges *et al*., 2000).

1.2.1. Antibiotic resistance along time

The first β-lactam antibiotic used to combat infections caused by *S. aureus* was penicillin in 1940. Florey and Chain showed its high efficiency against gram-positive bacteria (Chain *et al*., 1940), however penicillin had been discovered earlier in 1928 by Alexander Fleming (Fleming, 1929).

Although the mortality associated to *S. aureus* drastically decreased with the introduction of penicillin, it was only 2 years later that the first resistant strains appeared in hospitals and in the community (Rammelkamp and Maxon, 1942). Resistance to penicillin is mediated by the acquisition of a plasmid-borne gene (*blaZ*) that encodes for a β-lactamase protein. This protein is only synthesized in presence of β-lactam antibiotics and hydrolyses the β-lactam ring, inactivating the effect of the antibiotic (Kernodle, 2000).

To overcome the acquired resistance to penicillin several semi-synthetics antibiotics, derived from penicillin and resistant to β-lactamase action, were created. The first one was methicillin in 1960 (Rolinson *et al*., 1960), but one year later, the first methicillin-resistant *Staphylococcus aureus* (MRSA), carrying the *mecA* gene was reported (Jevons, 1961).

MRSA strains have not only acquired resistance to methicillin, but also against other classes of antibiotics that have completely different cellular targets, namely protein synthesis or nucleic acid synthesis, such as chloramphenicol or rifampicin, respectively (van Bambeke *et al*., 2003).

More recently, antibiotics with great efficacy against MRSA infections were introduced into clinical practice, such as linezolid in 2013 (Gu *et al*., 2013) and tigecycline and daptomycin in 2014 (Dabul and Camargo *et al*., 2014). However, some few resistant strains have already emerged.

1.2.2. MRSA, the most important nosocomial agent

Since the introduction of the antimicrobial chemotherapy in the 1930's, *S. aureus* has acquired many resistance traits. Methicillin resistance is the most important one and can be provided by one of two mechanisms: point mutations in specific chromosomal genes or horizontal transfer of an exogenous resistance gene. In this last mechanism, in which a single genetic element, the *mecA* gene, confers high level resistance to the major and more commonly prescribed class of antibiotics, the β-lactam antibiotics, such as penicillins, cephalosporins and carbapenemes (Grundman *et al*., 2006).

In the 1980s *S. aureus* became the major cause of nosocomial infections in hospitals, designated as Health care-Associated MRSA strains (HA-MRSA). In the 1990s as the infections caused by HA-MRSA strains tend to decrease, the Community-Associated MRSA (CA-MRSA) strains emerged, causing infections in healthy individuals with no risk factors and no previous contact with hospitals. The CA-MRSA presented some specific characteristics, namely enhanced virulence due to the capacity to produce specific toxins such as Panton-Valentine Leukocidin

(PVL) and decreased resistance levels. However, more recently, the CA-MRSA strains began to also appear in hospitals, and the distinction between HA and CA-MRSA is progressively blurring. In fact, CA-MRSA are now endemic in many US hospitals (de Lencastre *et al*., 2007a; Vandenesch *et al*., 2003).

1.2.3. Resistance to β-lactam antibiotics

Bacteria have developed a variety of responses to the challenge of β-lactam antibiotics. In order to prevent the access of the drug to its target, different strategies are adopted by bacteria cells: mutations in the genes that encode the β-lactam's targets, acquisition of β-lactamases (β-lactam hydrolytic deactivating enzymes), expression of protein inhibitors of the last enzymes, acquisition and activation of exporter proteins, removal of porin proteins of the cell membrane or modification of the cell wall (Fisher *et al*., 2005).

The targets of β-lactam antibiotics are the Penicillin-Binding Proteins (PBPs) that are involved in the last stages of peptidoglycan biosynthesis (van Bembeke *et al*., 2003). This class of antibiotics inhibit bacteria proliferation due to the fact that its ring is a structural analogue of the natural substrate of PBPs, the D-alanyl-D-alanine carboxy-terminus of the peptidoglycan pentapeptide (Tipper and Strominger, 1965). The β-lactam ring acylates the PBPs, forming a stable acyl-enzyme complex, in this way inactivating the PBPs by preventing them to bind to peptidoglycan (Yocum *et al*., 1979) (figure 1.1). The native enzymatic activity of PBPs includes the hydrolysis of the D-ala-D-ala bond of peptidoglycan and the formation of a new peptide bond between the fourth D-alanine residue and the terminal glycine residue of the bridge of the adjacent stem peptide.

β-lactam antibiotics are inactivated by β-lactamases that bind covalently to the β-lactam ring and hydrolyze its amide bond. These enzymes have amino acid sequence homology with PBPs and peptidases (Medeiros, 1997).

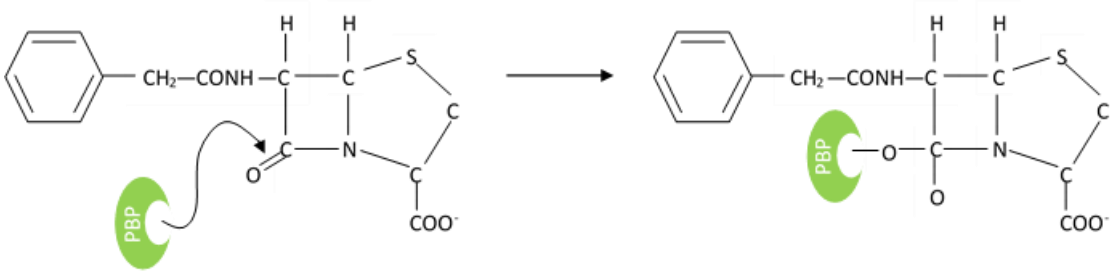

Figure 1.1 β-lactam antibiotic mechanism of action. The PBP present in the cell wall recognize the drug, analogous of its natural substrate, and bind to it, being inactivated.

1.2.3.1. Peptidoglycan biosynthesis

The peptidoglycan biosynthesis can be divided into three phases. The first one occurs in the cytoplasm with the synthesis of the nucleotide sugar-linked precursors UDP-MurNAc-pentapeptide and UDP-GlcNAc. The second takes place at the cytoplasmic membrane and leads to the synthesis of precursor lipid intermediates. At this stage the phospho-MurNAc-pentapeptide

of the UDP-MurNAc-pentapeptide is associated to bactoprenol, the membrane acceptor, giving rise to MurNAc-pentapeptide-pyrophosphoryl-undercaprenol (lipid I). Then, lipid I is transformed into lipid II by receiving a GlcNAc molecule from UDP-GlcNAc, generating GlcNAc-β-(1,4)-MurNAc-pentapeptide-pyrophosphoryl-undecaprenol. The final step of the peptidoglycan biosynthesis takes place at the cell wall with the polymerization of the disaccharide-peptide units into pre-existing peptidoglycan. At this point, the PBPs catalyze the transglycosylation and transpeptidation reactions that will result in the formation of the glycosidic and peptidic bonds of the peptidoglycan. The transglycosylation reaction leads to the elongation of glycan strands while in the transpeptidation reaction, the terminal D-ala-D-ala bond is cleaved, with the release of the terminal D-alanine, and a new peptide bond is formed between the penultimate D-alanine of a donor peptide and an amino group of the cross bridge of an acceptor peptide (Scheffers and Pinho, 2005). The basic unit of the peptidoglycan can be seen in figure 1.2.

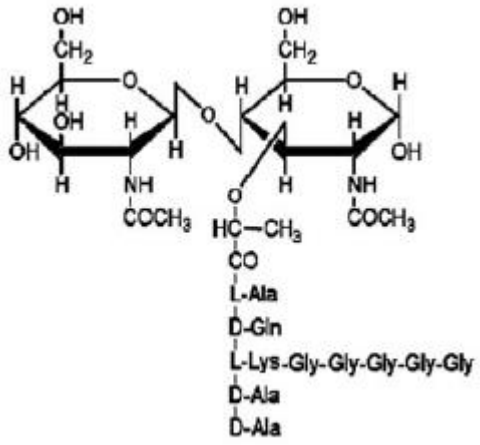

Figure 1.2 The basic unit of the peptidoglycan (Scheffers and Pinho, 2005).

1.2.3.2. The mechanism of resistance – *mecA* gene

The mechanism of resistance of MRSA strains involves the acquisition of *mecA* gene which encodes for Penicillin-Binding Protein PBP2A. The transpeptidation activity of this protein is redundant to the other Penicillin-Binding Proteins of *S. aureus*, however it has low affinity to β-lactams, and so, is able to takes over the peptidoglycan polymerization in the presence of the antibiotic (Fuda *et al*., 2005).

The *mecA* gene is exogenous to *S. aureus* and its origin is still unknown. One possibility is that *mecA* gene has evolved from a native gene of *Staphylococcus sciuri*, having been acquire by horizontal transfer (Couto *et al*., 1996). This bacteria colonizes the skin of domestic and wild animals and it is free of the penicillinase plasmid. The widely spread use of penicillin in veterinary medicine, may have contributed to the emergence of MRSA strains, through the selective pressure of the antibiotic (de Lencastre *et al*., 2007b).

The mobilization of *mecA* gene includes its incorporation into a mobile genetic element, the Staphylococcal Chromosome Cassette *mec* (SCC*mec*) (Katayama *et al*., 2003) that integrates

the *S. aureus* chromosome at a site-specific location (*attBscc*), situated near the origin of replication (Kuroda *et al*., 2001). This chromosomal cassette is bordered by recombinase genes (*ccr*A, *ccr*B or *ccr*C) that are responsible for the horizontal transfer of SCC*mec* (Hiramatsu *et al*., 2001). SCC*mec* is classified in many types, being the SCCmec type defined by the combination of the type of recombinase genes and the class of mec genes (Hiramatsu *et al*., 2013)

1.2.3.3. Major clones and MRSA epidemiology

A significant number of MRSA clonal lineages have emerged from Methicillin-susceptible *Staphylococcus aureus* (MSSA) strains with different genetic backgrounds that acquire SCC*mec* through independent acquisition events. It is thought that MSSA strains are able to acquire different forms of *mec* element, behaving as recipients for the SCC*mec* transference. In fact, the composition of this genetic element has been widely used to classify MRSA clones.

The first MRSA strain (NCTC10442) isolated in the United Kingdom in 1960 harbored SCC*mec* type I. This MRSA clone is nowadays known as the Archaic clone and it disseminated worldwide in the 1960s. In 1982, an MRSA strain (N315) was isolated in Japan that harbored SCC*mec* type II. This clone was called New York/Japan clone and spread worldwide (Ito *et al*., 2001). Three years later, in 1985, a MRSA strain (85/2082) containing SCC*mec* type III was discovered in New Zealand. Since the beginning of the 1990s that several MRSA clones harboring SCC*mec* type IV have disseminated worldwide (Vanderesch *et al*., 2003). In 2004, SCC*mec* type V was described in MRSA strain WIS, which was isolated in Australia. SCC*mec* type VI was first observed among MRSA isolates from Portugal and the prototype strain is called HDE288 (Oliveira *et al*., 2006), but more recently it has been described in MRSA isolates from other countries. SCC*mec* type VII was first discovered in MRSA strain TSGH-17 and has been observed in MRSA isolates from Taiwan (Takano *et al*., 2008).

At the present, 11 types of SCC*mec* are registered (IWG-SCC, 2009), and a large number of types is expected to appear during the next years.

1.2.4. Current identification techniques

Various identification techniques can be used to identify *S. aureus*. The most common are agglutination tests. The tube coagulase test detects the activity of coagulase enzyme but other species of staphylococci can also give positive results (Wichelhaus *et al*., 1999). The slide coagulase test detects a clumping factor that is attached to coagulase (Cookson *et al*., 1997), however negative results must be confirmed since many species of *S. aureus* do not have this clumping factor (Bannerman, 2003). Another assay that can detect the presence of clumping factor is the latex agglutination test that also detects protein A, a surface protein specific to *S. aureus* that is able to bind to the heavy chain of immunoglobulins. However, some MRSA strains produce undetectable levels of clumping factor or protein A (Kuusela *et al*., 1994). Futhermore, tests that include detection of the clumping factor may carry false-positives since other organisms produce this molecule (Peakock *et al*., 1999). DNase and heat-stable nuclease test with DNase plates can be performed to screen isolates. However coagulase-negative staphylococci (CoNS)

produce a great amount of DNase, so positives should be always confirmed (Barry *et al*., 1973). Commercial biochemical tests are also used to identify *S. aureus*, although they are slower and more expensive (ligozzi *et al*., 2002). Molecular tests are been used too, especially PCR to amplified a large range of targets but is extremely expensive due to a vast number of samples that is necessary to analyse. These techniques are the most reliable (Barski *et al*., 1996).

To evaluate the methicillin susceptibility different techniques exist, which I will give some examples. Dilution methods include agar dilution or broth microdilution strategies and both require the use of NaCl and growth of the bacterial culture (NCCLS, 2003). The Etest method also uses NaCl and agar and involves the growth and application of bacterial inoculum with a swab (Huang *et al*., 1993). Latex agglutination may be used for the detection of PBP2A and involves the PBP2a extraction (Nakatomi *et al*., 1998) but may be poorly reliable if the colonies used for the extraction of PBP2a were grown in a medium with NaCl (Brown *et al*., 2001). Molecular methods for the detection of *mecA* gene use radiolabelled or digoxigenin-labelled DNA probes (Archer *et al*., 1990). The detection of MRSA in screening samples is also possible, using solid agar media with or without enrichment media.

1.2.5. Current needs

The need to develop techniques that allow a faster diagnosis at an early stage of infection arises in order to allow an earlier treatment, as well as knowing what type of antibiotic can be administered.

Diagnostic techniques have been improved in the latest years, especially molecular diagnostics. These tests can be very cheap, fast and are fairly easy to accomplish. In addition, they can allow the bypass of an amplification step and possibly without bacterial culture.

1.3. Nanotechnology

Nanotechnology merges engineering and technology at the nanoscale and can be defined like the science that studies, manipulates and controls materials between 1 and 100 nanometeres (Debnath *et al*., 2009) (figure 1.3). It includes the development of techniques for molecular diagnostics, such as the specific and selective molecular identification of pathogenic organisms. In this context, nanotechnology provides a rapid diagnostic that allows an early action against the infectious agent (Leroy *et al*., 2010, Baptista *et al*., 2006).

The nanomaterials used in nanotechnology permit the development of new setups for detection of biomarkers (Perfézou *et al*., 2012) or DNA/RNA sequences of interest (Thaxton *et al*., 2006). Also, some of them are used as biosensors to cancer therapeutics and theragnostics agents (Singh *et al*., 2012) and for drug delivery (Barakat, 2009) (figure 1.3).

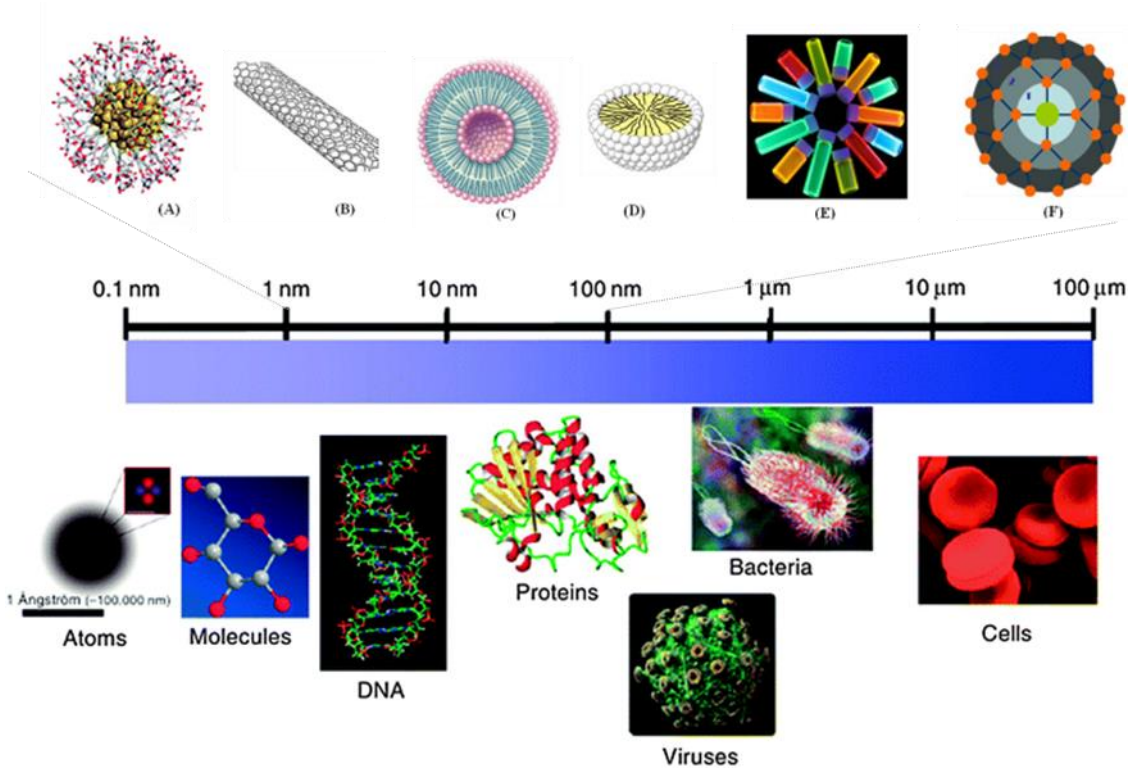

Figure 1.3 Examples of nanomaterials (A-F upper the scale) and comparison with chemical and biological reagents (lower the scale) in terms of size. The nanomaterials are comprised between 1 and 100 nm. A) gold-nanoparticle; B) carbon nanotube; C) liposome; D) micelle; E) quantum dot; F) dendrimer. Adapted from Marradi *et al*., 2010 and Joshi and Wang, 2010.

Nanomaterials have demonstrated their potentialities for biosensing application. High specific surface is one of the advantage of the nanomaterials in their use as biosensors, and provides high sensitivities and lowered detections limits. A biosensor can be defined by its biological or bioinspired receptor unit with unique specificities to corresponding analytes. The biological recognition is captured by transducers that translate the information into, for example, electrochemical, magnetic or optical signals (Holzinger *et al*, 2014).

1.3.1. Gold Nanoparticles

Gold nanoparticles (AuNPs) are widely and increasingly used for their potential on diagnostics. They are easily synthesized, in order to have controlled sizes and shapes (figure 1.4), and are extremely versatile, presenting great optical and physical properties such as intense colors or surface plasmon resonance (SPR), characteristics that are required to obtain a colorimetric result (Baptista *et al*., 2005).

SPR can vary with shape, size and composition of the AuNP (Hutter *et al*., 2004) and with the interparticle distance (Baptista *et al*., 2005, Sato *et al*., 2003). As the incident light reaches the AuNPs solution, all the conduction-band electrons at the surfaces of the AuNPs begin to oscillate together due to the electromagnetic field of the light. These oscillating electrons form dipoles that annul the electromagnetic fields of the same frequency. SPR is established when the oscillation frequency of the electrons at the surface of the AuNPs matches the frequency of the electromagnetic field of the light (Eustis and El Sayed, 2006).

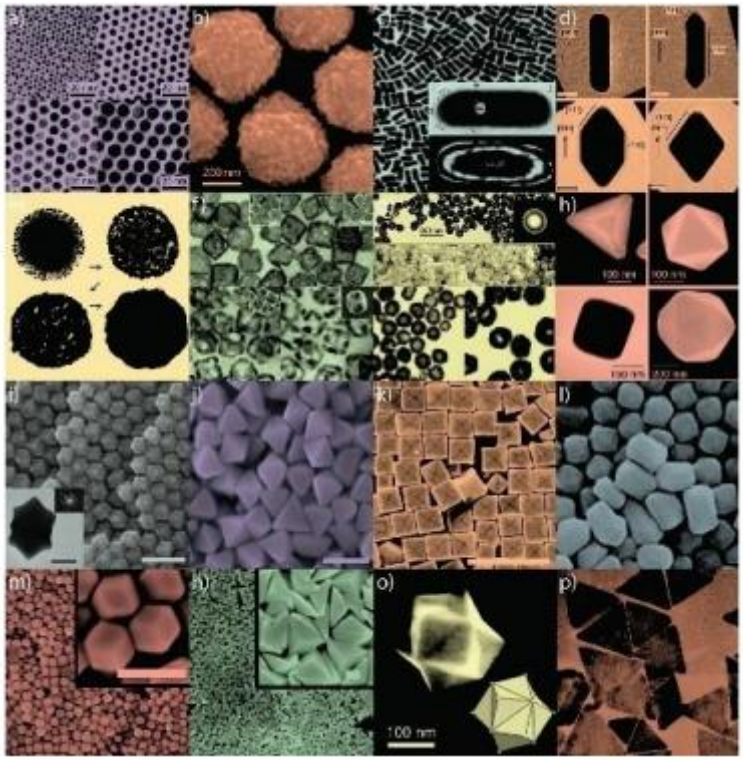

Figure 1.4 AuNPs of various sizes and shapes with potential application in biomedicine. Small (a) and large (b) nanospheres, (c) nanorods, (d) sharpened nanorods, (e) nanoshells, (f) nanocages/frames, (g) hollow nanospheres, (h) tetrahedra/octahedra/cubes/icosahedra, (i) rhombic dodecahedra, (j) octahedra, (k) concave nanocubes, (l) tetrahexahedra, (m) rhombic dodecahedra, (n) obtuse triangular bipyramids, (o) trisoctahedra, and (p) nanoprisms (Dreaden *et al*., 2012).

Usually, for spherical AuNPs with 14 nm of diameter, the maximum SPR absorbance peak is localized at approximately 520 nm, conferring the AuNPs a strong red colour (Huang *et al*., 2007). As the size of the AuNPs increases, their colour tends to blue and the SPR peak suffers a shift to higher wavelengths, to the region of 600 nm, approximately. The same phenomenon is observed upon particle aggregation: when AuNPs associate and start to behave like a larger nanoparticle, their optical properties change accordingly and a shift to blue colour occurs (Sato *et al*., 2005).

1.3.1.1. Synthesis

The nanomaterials can be synthesized by one of two concepts: top-down and bottom-up. Top-down methods include techniques such as lithography (Acikgoz *et al*., 2011), laser ablation (Mafuné *et al*., 2001) and focused ion beam (Shahmoon *et al*., 2010). These approaches tend to be slow and require the use of expensive equipment (Mühlig and Rockstuhl, 2013). Bottom-up methods relies on the production of nanomaterials from their precursors via self-assembly, requiring simple laboratory setup and tending to be simpler and faster than top-down methods (Grzelczak *et al*., 2010). Both concepts have being used to produce AuNPs.

However, the synthesis of AuNPs for applications in non-crosslinking methods (see section 1.3.2.) has been optimized by chemical reduction. Through addition of a reducing agent, sodium citrate, to a solution of chloroauric acid, Au^{3+} ions are reduced to neutral gold atoms, Au^{0}. Being the capping agent, sodium citrate controls the shape, morphology and synthesis rate of the AuNP.

Moreover, it is responsible for preventing aggregation of the AuNPs by electrostatic stabilization or by steric hindrance (Richards *et al*., 2005).

If the aim is to functionalize AuNPs (see section 1.3.1.2.) with ssDNA, the nanoparticles must be hydrophilic. The citrate reduction method (Turkevich *et al*., 1951) produces hydrophilic spherical AuNPs with 10 to 30 nm diameter. As stated above, in this method, sodium citrate acts both as a reducer and as a capping agent. By varying the molecular ratio of sodium citrate and gold salts, AuNPs of different diameters can be obtained, since higher concentrations of citrate lead to the formation of smaller particles and lower concentrations lead to the formation of larger particles. This phenomenon is due to the fact that, during the synthesis reaction, the diameter of the AuNPs increases until saturation by sodium citrate occurs (Ji *et al*., 2007).

This method gives rise to stable nanoparticles with negative charge, due to citrate capping, stabilized by electrostatic repulsion due to adsorption of sodium citrate to the surface of the AuNPs, a great advantage for the subsequent modification of the surface of the nanoparticle (Kumar *et al*., 2012).

1.3.1.2. Functionalization

AuNPs can be functionalized with a wide list of organic ligands (see figure 1.5) in order to produce hybrid particles with enhanced functionality. With the appropriate ligand, nanoparticles can be used for gene silencing, drug delivery, colorimetric assays, sensing systems, imaging, and intracellular targeting, among others.

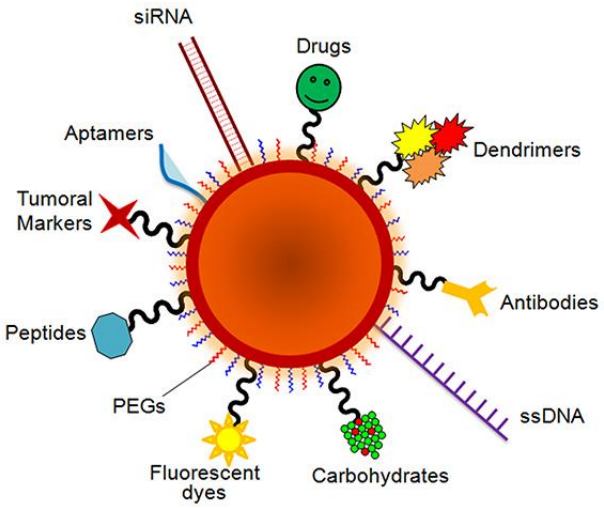

Figure 1.5 Schematic representation of an AuNP with various ligands (Conde *et al*., 2014).

Thiol groups have higher affinity for gold than sodium citrate, resulting in a quasi-covalent bond (Love *et al*., 2005) that stabilizes AuNPs against aggregation by salt induction (Sperling *et al*., 2010).

The functionalization of nanoparticles with 5'-thiol-modified oligonucleotides by salt-aging consists on the successive addition of salt to the solution of modified oligonucleotides and AuNPs (figure 1.6). The salt reduces the electrostatic repulsion between oligonucleotides and AuNPs that

are both negatively charged. Surfactants like SDS are also used to improve the stability of the system. Thus, high concentrations of salt are needed to induce the aggregation of au-nanoprobes. A sonication step is performed after each salt addition in order to disrupt the interactions between the oligonucleotide bases. In this way, the surface of AuNP becomes more available for additional oligonucleotides to bind (Hurst *et al*., 2006).

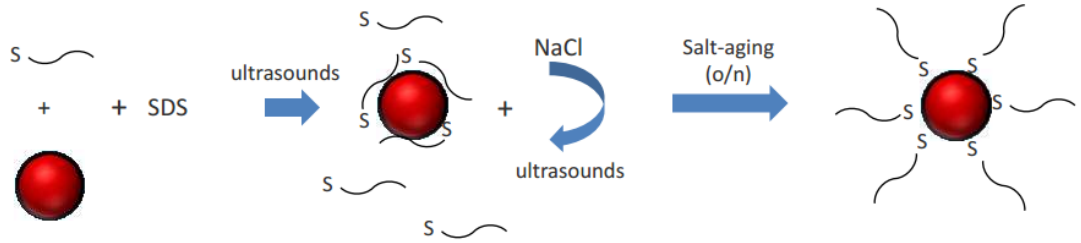

Figure 1.6 Schematic representation of functionalization of AuNPs with 5'-thiol-modified oligonucleotides by salt-aging (adapted from Hurst *et al*., 2006).

1.3.2. Non-crosslinking method

1.3.2.1. DNA/RNA detection Gold nanoprobes

The non-crosslinking method used in this work was designed by Baptista and co-workers (figure 1.7). If the Au-nanoprobes hybridize with complementary targets, the formation of heteroduplexes will provide stability to the Au-nanoprobes against salt-induced aggregation since the heteroduplex structure offers protection to the negatively charged backbones by steric hindrance. The stabilization is obtained when the electrostatic repulsions and the interparticle distance between AuNPs do not decrease (Baptista *et al*., 2005).

If the target present in the solution is a non-complementary target, the Au-nanoprobes will not stabilize and aggregation will occur in response to an increase of ionic strength upon salt addition. This aggregation phenomenon results in a change of color of the solution from red to blue that can be quantified with a spectrophotometer.

The ratio between Abs_{525nm} and Abs_{600nm} is commonly used to analyze and evaluate surface plasmon resonance variations. Abs_{525nm} represents the maximum absorbance of the dispersed Au-nanoprobes, while Abs_{600nm} represents the maximum absorbance for the aggregated Au-nanoprobes (Costa *et al*., 2010).

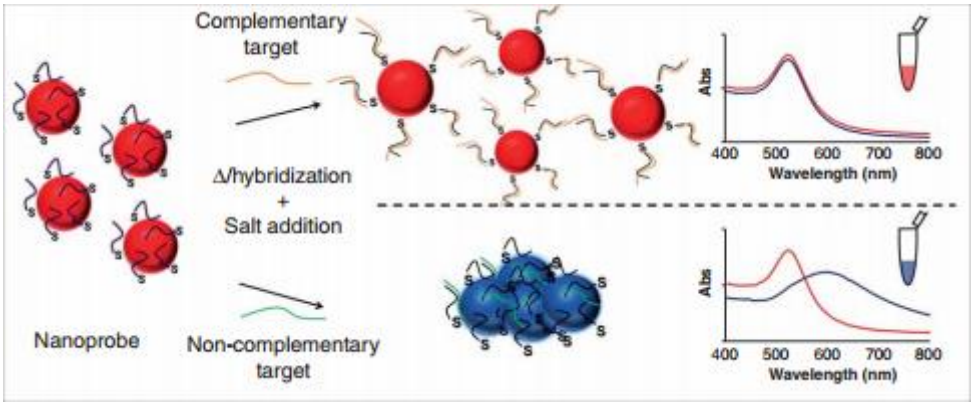

Figure 1.7 Non-crosslinking colorimetric assay using Au-nanoprobes for identification of nucleotides sequences (adapted from Larguinho *et al*., 2012).

An Abs_{525nm}/Abs_{600nm} ratio of 1 corresponds to equivalent amounts of dispersed and aggregated Au-nanoprobes in the solution. Ratios over 1 are associated with a higher amount of dispersed Au-nanoprobes in comparison to aggregated ones, meaning that hybridization of the Au-nanoprobes with a complementary target and consequent stabilization occurred. On the other hand, a ratio value below 1, means that the amount of aggregated Au-nanoprobes is higher due to the presence of a non-complementary target (Larguinho *et al*., 2014). The trapezoidal rule can also be used to calculate the "areas under the curve" to both fractions dispersed and aggregated, originate a ratio between them (Conde *et al*., 2010).

To perform the colorimetric assay, it is more advantageous to use divalent salts, such as $MgCl_2$, since they are capable of inducing aggregation of the nanoparticles at lower concentrations than monovalent salts (Duguid *et al*., 1995).

Other important parameters have to be taken into account for the optimization of the non-crosslinking colorimetric assay: the nanoprobe concentration in the solution affects the stability assays, as it is related with the interparticle distance; the pH of the solution will influence the hybridization efficiency and target:probe specificity; the oligonucleotide density on the surface of AuNP will also influence the hybridization efficiency (Sun *et al*., 2009).

Once the optimal conditions of stability and hybridization are defined, the non-crosslinking method optimized by Baptista and co-workers can be used for colorimetric assays.

1.4. Thesis Scope

The molecular methods for detect MRSA infections involve carrying out a DNA amplification step result in high costs as also important hours. The huge emergence of the developing of new diagnostics techniques with less time-consuming, less costs and reliable makes it an important issue that has direct implication in human health.

The main objective of this thesis is to develop a molecular method of diagnostics, using gold nanoprobes and based on non-crosslinking method, that permits the identification of the presence of *mecA* gene, responsible for the resistance to β-lactams antibiotics. In pursuit of that this is the set objectives of this study:

1. Selection of target sequences;

2. Au-nanoprobes synthesis and characterization;

3. Extraction and purification of plasmid DNA from selected strains;

4. Amplification by PCR of selected fragments;

5. Extraction and purification of genomic DNA from selected strains;

6. Extraction and purification of RNA from selected strains. Optimization of extraction protocol for ease at point-of-care;

7. Au-nanoprobes for sample analysis.

2. Materials and Methods

2.1. Materials

2.1.1. Equipment

Table 2.1 Equipment

Equipment	Manufacturer
DLS, SZ-100	Horiba
FastPrep FP120	Thermo Electron
Gel Doc XR+ Molecular Imager System	Bio-Rad
Microfuge 3-16K	Sartorius, Sigma
Microfuge 1-14	Sartorius, Sigma
Microplate reader Infinite M200	Tecan
Peltier Thermal Cycler DNA Engine	Bio-Rad
Power supply electrophoresis	BioRad
Programmable Thermal Controller PTC-100	MJ Research, Inc
Sonoreactor UTR200	Hielscher
Speed Vac	Savant
Ultrasonic bath Elmasonic S10H	Elma
UV-Vis Spectrophotometer NanoDrop ND1000	NanoDrop Technologies
UV-Vis Spectrophotometer UV mini 1240	Shimadzu

2.1.2. Chemical Reagents

All the chemical reagents used in this work were purchased from Sigma, Merck, Fluka, Invitrogen, Liofilchem and Panreac, with the highest purity available.

2.1.3. Biological Reagents

All the primer and target DNA fragments were ressuspended in sterile and filtrated water to achieve a concentration of 100 pmol and were stored at -20ºC. The treatment of the thiol-modified oligonucleotides is explained in “Functionalization of AuNPs” method.

2.1.3.1. Oligonucleotides sequences

Table 2.2 Oligonucleotides sequences

Name	Sequence (5'-3')	Description
pmecAfw	GAACAGCATATGAGATAGGC	Primer
pmecArv	ACTGCATCATCTTTATAGCC	Primer
mecA_probe	Thiol-ACTAATGAAACAGAAAGTCG	Probe
mecA_target	CTTTTCCTAGAGGATAGTTACGACTTTCTGTTTCATTAGT	Target
mecA_probeV2	Thiol-CCT AAT AGA TGT GAA GTC GC	Probe
mecA_targetV2	ATC CTC TAG AAA AAG CGA CTT CAC ATC TAT TAG G	Target
pfalci18SF3	CAG ATG TCA GAG GTG AAA TTC	Primer
pfalci18SB3	CAT GCA TCA CCA TCC AAG AAA TCA A	Primer

2.1.3.2. Molecular Biology reagents

Table 2.3 Molecular Biology reagentes.

Product	Producer
dNTPs mix	Fermentas
DreamTaq Buffer	Fermentas
DreamTaq polymerase	Fermentas
GelRed	Biotium
GeneRuler DNA Ladder Mix	Fermentas
Oligonucleotides	StabVida
RNA protect	Qiagen
RNase A	Fermentas

2.1.4. Other materials

Table 2.4 Other materials.

Product	Producer
Acrodisc 32 mm Syringe Filter with 0.2µm Supor Membrane	PALL
Dialysis Tubing – Visking Code DTV03500.02.00	Medicell Membranes Ltd
LoBase Polystyrene microplates 384	Greiner Bio-One
NAP-5 columns Sephadex G-25 DNA Grade	GE Healthcare
Quartz Absorption Cell 105.202-QS	Hellma

2.1.5. Solutions

- AGE I:
  - 2% (w/v) SDS
  - 10 mM phosphate buffer pH 8
  - The solution was filtrated and stored at 4ºC
  - The solution was warmed to 25ºC before use, to dissolve the SDS.
- AGE II:
  - 1.5M NaCl
  - 0.01% (w/v) SDS
  - 10 mM phosphate buffer pH 8
  - The solution was filtrated and stored at 4ºC
  - The solution was warmed to 25ºC before use, to dissolve the SDS.
- Alkaline Lysis I (AL I):
  - 50 mM Glucose
  - 10 mM Tris-HCL pH 8
  - 1 mM EDTA pH 8
  - The solution was autoclaved and stored at 4ºC.
- Alkaline Lysis II (AL II):
  - 200 mM NaOH
  - 1% (w/v) SDS
  - The solution was always freshly prepared.
- Alkaline Lysis III (AL III):
  - 3M sodium acetate
  - The pH was adjusted to 5 with glacial acetic acid
  - The solution was stored at 4ºC
- Luria Bertani (LB) medium:
  - 1% (w/v) tryptone
  - 0.5% (w/v) yeast extract
  - 171 mM NaCl
  - The pH was adjusted to 7, the medium was autoclaved and stored at 4ºC.
- Phosphate Buffer 10 mM pH 7 0.1M Nacl:
  - 5.77 mM Na_2HPO_4
  - 4.23 mM NaH_2PO_4
  - 0.1 M NaCl
  - The Buffer was autoclaved and stored at 4ºC
- Phosphate Buffer 10 mM pH 8:
  - 9.32 mM Na_2HPO_4
  - 0.68 NaH_2PO_4
  - The Buffer was autoclaved and stored at 4ºC.

- Phosphate Buffer 10 mM pH8 0.1M NaCl:
  - 9.32 mM Na_2HPO_4
  - 0.68 NaH_2PO_4
  - 0.1 M NaCl
  - The Buffer was autoclaved and stored at 4ºC

2.2. Methods

2.2.1. Plasmid DNA Extraction

1. 10 mL of LB medium with 100 µg/mL ampicillin were inoculated with plasmids of cloned *mecA* gene from *S. aureus* and cloned 18S ribosomal gene of *Plasmodium falciparum* and incubated overnight at 37ºC with agitation.
2. The culture was transferred to 1.5 mL tubes and centrifuged at 6660 x g for 15 minutes.
3. The supernatant was discarded, the pellet were resuspended in 150 µL of AL I solution and the sample was incubated on ice for 5 minutes.
4. 300 µL of AL II solution were added, the sample was homogenized gently by inversion and then incubated on ice for 5 minutes.
5. 225 µL of ALIII solution were added, the sample was homogenized by inversion and then incubated on ice for 30 minutes.
6. The lysate was centrifuged at 12500 x g for 30 minutes with soft start.
7. The supernatant was transferred to a clean tube and 2 volumes of ice-cold Absolut Ethanol were added.
8. The DNA was precipitated at -20ºC for 2 hours and centrifuged at 12500 x g for 10 minutes.
9. The supernatant was removed and the precipitate was washed with 1 volume of ice-cold 70% Ethanol and centrifuged at 12500 x g for 15 minutes.
10. The supernatant was discarded and the pellet was dried using a vacuum concentrator.
11. The DNA was ressuspended in 200 µL of sterile and filtrated water.
12. RNase A was added to a final concentration of 40µg/mL and incubated overnight at 37ºC.
13. 1 volume of phenol was added and the sample was thoroughly mixed for 1 minute.
14. After centrifugation at 12500 x g for 5 minutes the aqueous phase was transferred to a clean tube.
15. 1 volume of Phenol/Isoamyl Alcohol (24:1) was added and the sample was thoroughly mixed for 1 minute.
16. The sample was centrifuged at 13000 rpms for 5 minutes and the aqueous phase was transferred to a clean tube.
17. The DNA was precipitated with 2 volumes of absolute ethanol and washed with 1 volume of 70% Ethanol as in steps 7 to 10.
18. The DNA was ressuspended in 100 µL of sterile and filtrated water.
19. The sample was stored at -20ºC.

2.2.2. Genomic DNA Extraction

1. 1 mL of an overnight culture of COL and NCTC8325 *S. aureus* strains was centrifuged at 12500 x g for 2 minutes and the supernatant was removed.
2. The cell pellet was ressuspended in 100 µL of Tris, 1 µL of lysostaphin and 3 µL of RNase and incubated at 37ºC for 1 hour.
3. To complete the cell lysis procedure 600 µL of Nuclei Lysis Solution were added and gently homogenized.
4. The lysate was incubated at 80ºC for 5 minutes and then cooled to room temperature.
5. 200 µL of Protein Precipitation Solution were added to the RNase-treated cell lysate and the solution was vigorously mixed (vortex) for 20 seconds.
6. The sample was incubated on ice for 10 minutes and centrifuged at 13000 x g for 30 minutes at 4ºC.
7. The supernatant was transferred to a clean tube containing 600 µL of room temperature isopropanol and the contents were gently mixed by inversion until thread-like strands of DNA form a visible mass.
8. The sample was incubated for 15 minutes at room temperature and centrifuged at 13000 x g for 30 minutes at 4ºC.
9. The supernatant was removed and the DNA pellet was washed with 600 µL of 70% Ethanol.
10. The sample was centrifuged at 13000 x g for 15 minutes at 4ºC and the ethanol was aspirated.
11. The pellet was air-dried for 15 minutes and 100 µL of TE 1x were added.
12. The sample was stored at 4ºC.

2.2.3. Amplification of *mecA* gene and *P. falciparum* 18S RNA fragments by Polymerase Chain Reaction

2.2.3.1. Reaction Mixture

- 1x DreamTaq Buffer
- 0.2 µM primer rv
- 0.2 µM primer fw
- 0.2 mM dNTPs mix
- 25 mU/µL DreamTaq polymerase
- 4 ng/µL template

Sterile and filtrated water was added to the reaction mixture to the desired final volume. All the reagents were added in order to attain these final concentrations. A control reaction was performed without target which was replaced by sterile and filtrated water.

2.2.3.2. Reaction Program

mecA gene products:

1. 5 minutes, 95ºC Pre-Denaturation
2. 30 seconds, 95ºC Denaturation
3. 30 seconds, 59ºC Annealing
4. 90 seconds, 72ºC Extension
5. The steps 2 until 4 were repeated 30 times
6. 10 minutes, 72ºC Final extension

P. falciparum products:

1. 5 minutes, 95ºC Pre-Denaturation
2. 30 seconds, 95ºC Denaturation
3. 30 seconds, 58ºC Annealing
4. 30 seconds, 72ºC Extension
5. The steps 2 until 4 were repeated 30 times
6. 3 minutes, 72ºC Final extension

2.2.4. Purification of PCR products

2.2.4.1. Ethanol precipitation

1. The PCR product was precipitated with 2 volumes of ice-cold Absolut Ethanol, mixed by inversion and incubated at -20ºC overnight.
2. The sample was centrifuged at 15500 x g and 4ºC for 20 minutes and the supernatant was discarded.
3. The PCR product was washed with 1 volume of 70% Ethanol and centrifuged at 15500 x g and 4ºC for 15 minutes.
4. The supernatant was removed and the pellet was air-dried on a speed-vac.
5. The pellet was ressuspended in 100 µL of sterile and filtrated water.
6. The samples were stored at -20ºC.

2.2.4.2. Dialysis

1. The PCR products were introduced in the tampion of 1.5 mL tubes that were cut off of the tubes.
2. A dialysis membrane of 3500 da was used to cover the tampion and the samples were introduced in a beaker with miliQ water with agitation overnight.
3. The samples were transferred to new tubes and stored at -20ºC.

2.2.5. DNA fragmentation

1. The DNA samples were introduced in 1.5 mL tubes with a final DNA concentration of approximately 300 ng/µL.

2. The samples were sonicated with the help of a sonoreactor, during 6 minutes at 100% ultrasonication amplitude.

3. The samples were stored at 4ºC.

2.2.6. RNA Extraction

1. 50 mL of TSB medium were inoculated with an overnight culture in order to obtain an initial OD_{620nm} of 0.01.

2. The culture was incubated at 37ºC with vigorous shaking until the OD_{620nm} reached 0.7-1, corresponding to the mid-exponential phase of growth.

3. 10 mL of the culture were transferred to a 50 mL tube and the double volume of 20 mL of RNA protect was added.

4. The mixture was thoroughly homogenized using a vortex for 10 seconds and incubated at room temperature for 5 minutes.

5. The cells were pelleted by centrifugation at 6660 x g and 4ºC for 20 minutes and the supernatant was discarded.

6. The pellets were stored at -80ºC.

7. While the pellet was still frozen, 2 mL of Trizol were added. The pellet was ressuspended using the vortex.

8. The 2 mL of Trizol/ressuspended cells was divided into two 2 mL screw cap tubes with silica beads of 0.1 mm.

9. The cells were lysed in a FastPrep apparatus (speed setting=6 and time setting=40 seconds), a high-speed benchtop homogenizer.

10. After cell disruption, the sample was left at room temperature for 10 minutes. RNA is stable in trizol which deactivates RNases.

11. RNA extraction was achieved by adding 1/5 volume of Chloroform followed by vigorous shaking (vortex) and phase separation at room temperature for 5 minutes.

12. The sample was centrifuged at full speed for 15 minutes and the aqueous upper phase was transferred to a clean 1.5 mL tube.

13. Isopropanol was added to the aqueous phase to a final concentration of 70%, the mixture was homogenized by inversion and then incubated at room temperature for 10 minutes.

14. The sample was centrifuged at full speed for 15 minutes and the supernatant was removed, leaving approximately 100 µL covering the pellet.

15. 800 µL of 80 % ethanol were added to remove salts and the sample was slightly vortexed to release the RNA pellet from the bottom of the tube.

16. The sample was centrifuged at full speed for 2 minutes and the supernatant was removed as in step 14.

17. Washing step 15 was repeated.

18. The sample was centrifuged at full speed for 2 minutes and the supernatant was completely removed.

19. The tubes were air-dried for 10 minutes and 25 µL of DEPC water were added to the pellet.

20. The pellets were ressuspended at room temperature for 10 minutes and stored at -80C.

2.2.7. Synthesis of AuNPs

1. All glass material was washed by immersion with *aqua regia* ($HCl:HNO_3$, 3:1) overnight and later with miliQ water (18.2 MΩ.cm at 25 °C).

2. A 500 mL round bottom flask with 250 mL of 1 mM HAuCl4 was boiled with vigorously stirring until reflux was reached.

3. 25 mL of 38.8 mM sodium citrate were added and 20 minutes later the colloidal solution was cooled at room temperature.

4. The colloidal solution was filtered using a 0.2 µm acrylic membrane and then stored in the dark, at room temperature.

2.2.8. Transmission Electronic Microscopy (TEM) analysis

The samples of AuNPs were sent to Instituto de Ciência e Engenharia de Materiais e Superfícies (ICEMS/IST) for TEM analysis. The preparation of samples involved the depositing of 10 µL of the previously prepared colloidal solution containing the AuNPs in carbon copper grids, washing twice with 10 µL of MiliQ water and them air dried. The TEM analyzis was performed with a HITACHI H-8100 microscope operated at 200 kV. The size and shape of the AuNPs were determined by analyzing the TEM pictures using the imaging software Carnoy 2.0.

2.2.9. Functionalization of AuNPs

2.2.9.1. Oligo nucleotides preparation

1. The thiol-modified oligonucleotide was ressuspended in 100 µL of 1M DTT and the sample was incubated at room temperature for 3 hours.

2. Sterile and filtrated water was added to a final concentration of 0.1M DTT.

3. One volume of the thiol-modified oligonucleotide was extracted with two volumes of ethyl acetate and the sample was gently mixed.

4. The sample was centrifuged at 14460 x g for 5 minutes and the organic upper phase was discarded.

5. Steps 3 and 4 were repeated twice.

6. The aqueous phase was purified on a NAP-5 column and eluted with 10 mM phosphate buffer pH 8.0.

7. The thiol-modified oligonucleotide was quantified by UV/Vis spectroscopy using NanoDrop.

2.2.9.2. Au-nanoprobes synthesis

1. The purified thiol-modified oligonucleotide was mixed with a solution of approximately 15 nM AuNPs to a theoretical ratio of 1:200 (AuNPs:Oligos).
2. AGE I solution was added to a final concentration of 10 mM phosphate buffer pH 8.0 and 0.01% (w/v) SDS and the sample was incubated 20 minutes at room temperature.
3. Aliquots of AGE II solution were added in order to increase the ionic strength of the solution, to attain final concentrations of 0.05, 0.1, 0.2 and 0.3M NaCl. The aliquots were added every 20 minutes followed by 10 seconds in an ultra-sounds bath.
4. After all the additions the solution was stored at room temperature overnight.
5. The obtained Au-nanoprobe sample was aliquoted in 2 mL tubes and centrifuged at 15500 x g for 40 minutes and the supernatant was discarded.
6. The pellets were washed three times with 10 mM phosphate buffer pH 8.0 and twice with 10 mM phosphate buffer pH 8.0 0.1M NaCl.
7. The pellets were added together, resulting in a final concentration of functionalized AuNPs of 13 nM.

2.2.10. DLS analysis

The hydrodynamic radius of Au-nanoparticles and Au-nanoprobes was determined with Dynamic Light Scattering. A volume of 500 µL of approximately 2.5 nM Au-nanoparticles and Au-nanoprobes was measured.

DLS analysis was performed in Departamento de Química (FCT/UNL).

2.2.11. Nanoprobes Stability Assays

1. A solution containing a final concentration of Au-nanoprobe of 2.5 nM, and 10 mM phosphate buffer pH 7.0, 0.1M NaCl was heated during 5 minutes at 95ºC, cooled to room temperature and incubating at this temperature during 5 minutes.
2. Increasing concentrations of MgCl2 was added to the Au-nanoprobe sample to increase the salt concentration and reaching a total volume of 30 µL.
3. 20 minutes after salt addition all the samples were introduced in a microplate well and UV-visible spectroscopic measurements were registered in a microplate reader.

2.2.12. Non-crosslinking Detection Assays

1. The amount of target needed for a detection assay was added to a solution of 2.5 nM Au-nanoprobe and 10 mM phosphate buffer pH 7.0, 0.1M NaCl. In parallel a blank solution without target was prepared.
2. All samples were heated for 5 minutes at 95ºC, cooled down to room temperature and incubating at this temperature for 5 minutes.
3. $MgCl_2$ was added to the samples in order to reach the minimum salt concentration necessary to induce aggregation, reaching a total volume of 30 µL.

4. 20 minutes after salt addition all the samples were introduced in a microplate well and UV-visible spectroscopic measurements were registered in a microplate reader.

3. Results and Discussion

As the prevalence of MRSA colonization and infection has increased after the introduction of β-lactam antibiotics in hospitals and in the community, rapid and accurate detection systems of MRSA have been developed.

In this work the non-crosslinking method based on the colorimetric changes of Au-nanoprobes induced by the addition of salt was used for the detection of MRSA. To achieve this, a target sequence of the gene that confers resistance to methicillin, *mecA* gene, was chosen.

3.1. Design of primers and probes

Two primers, forward and reverse, of 20 nucleotides and with a GC content comprised between 40 and 50% were designed for the amplification of a consensus and relatively stable region of *mecA* gene with 334 bp.

For the colorimetric detection two probes were chosen, mecA and mecA_V2, both localized close to the middle of the target sequence, distant from the primers. As for the primers, both probes were 20 nucleotides long with a GC content comprised between 40 and 50%. The target region, primers and probes are schematically represented in figure 3.1.

The sequences of all the oligonucleotides were chosen with the help of NUPACK nucleic acid package (available online at www.nupack.org/design/new) and analyzed with the help of Nucleotide BLAST (Basis Local Alignment Search Tool) (available online in blast.ncbi.nlm.nih.gov/Blast.cgi). The NUPACK tool allowed choosing primers and probes that are not prone to self-annealing and with a free energy of secondary structures of 0.00 kcal/mol. The Nucleotide BLAST algorithm allowed to search for sequences in the database with which the probes could hybridize. Both probes only present 100% complementarity to sequences from the genomes of MRSA strains indicating that both probes are specific for MRSA detection.

In addition, mecA probe is complementary to the antisense chain of *mec*A gene sequence, while mecA_V2 probe is complementary to the sense chain of the target.

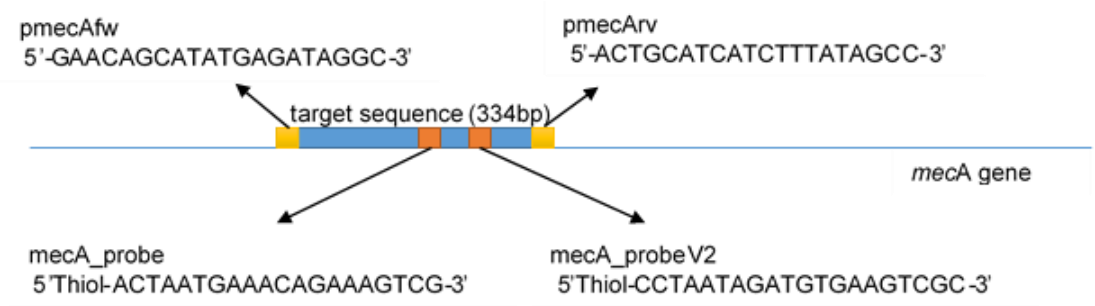

Figure 3.1 Schematic representation of the target region of the *mecA* gene and primers (in yellow) and probes position (in orange).

3.2. Preparation of targets

During the development of this work, DNA fragments of *mecA* gene were required as well as DNA fragments with no complementarity either to *mecA* gene or to the probes, with the pursuit of serving as non-complementary targets for the non-crosslinking assays.

Firstly, plasmid DNA (pDNA) was extracted by the alkaline lysis method from plasmids of cloned *mecA* gene from *S. aureus* and of cloned 18S ribosomal gene from *Plasmodium falciparum*, both kindly provided by PhD student Bruno Veigas. PCR reactions using pmecA and pfalci specific primers were performed as suffered minor optimizations in the annealing temperature, so that there is no nonspecific products. In a second phase, genomic DNA (gDNA) of *S. aureus* strains COL (MRSA) and NCTC8325 (MSSA) was extracted using a commercial kit and finally RNA extraction from the same *S. aureus* strains was obtained using a Trizol based method.

The success of the all the extractions procedures and the PCR products was evaluated by electrophoretic analysis in agarose gel (figure 3.2) and by UV-vis spectroscopy - a single absorbance peak at 260 nm was obtained indicating that the nucleic acids were not contaminated. The nucleic acids concentrations were calculated using Nanodrop ND-1000 and then the targets were used for Au-nanoprobes detection assays. The PCR products were sequenced and the presence of the target sequence of *mecA* gene was confirmed as also the non-complementarity of *P. falciparum* products to the probes (Appendix A1).

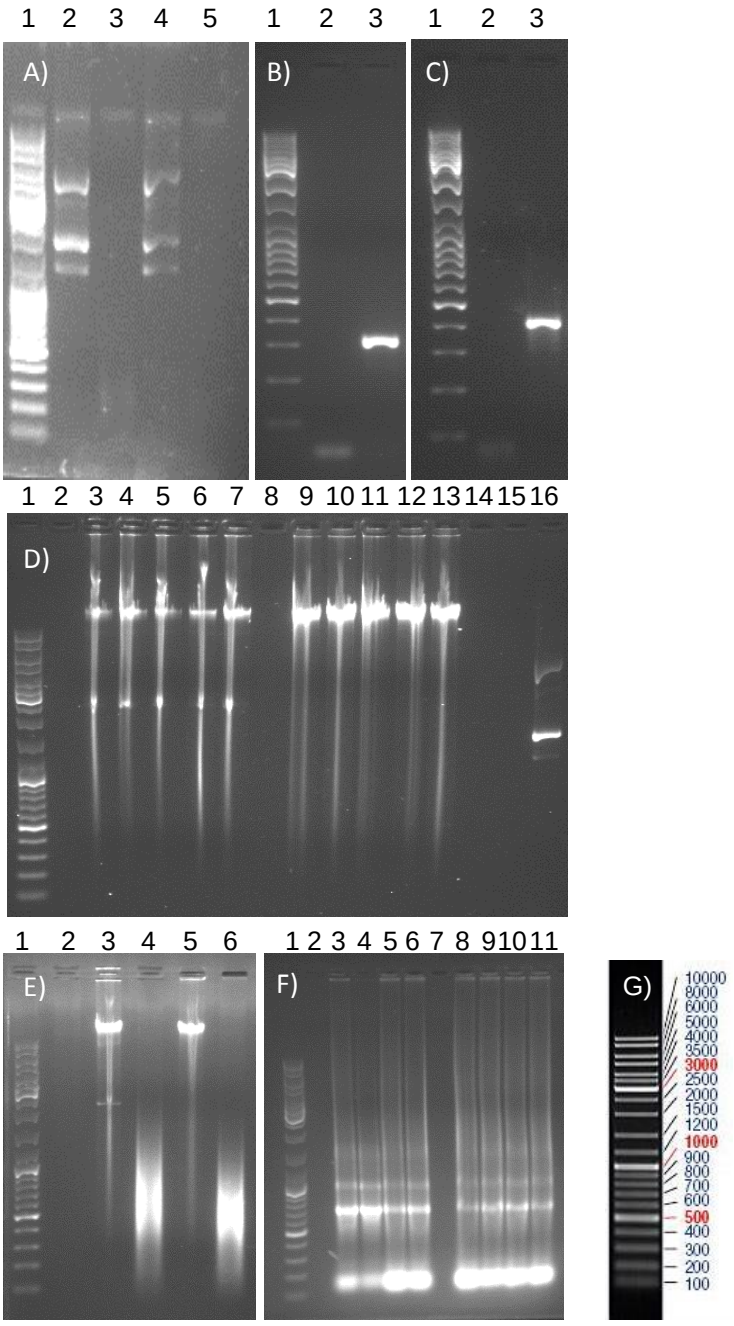

Figure 3.2 Electrophoretic analysis in 1% agarose gel. A) pDNA: lane 2 - mecA plasmid, lane 3 - sonicated mecA plasmid, lane 4 - falci plasmid, lane 5 - sonicated falci plasmid. B) mecA PCR product in lane 3, lane 2 is the negative control. C) falci PCR product in lane 3, lane 2 is the negative control. D) gDNA: COL gDNA in lanes 3-7, NCTC8325 gDNA in lanes 9-13, mecA pDNA in lane 16. E) gDNA: COL gDNA in lane 3, sonicated COL gDNA in lane 4, NCTC8325 gDNA in lane 5, sonicated NCTC8325 gDNA in lane 6. F) RNA: COL RNA in lanes 3-6, NCTC8325 RNA in lanes 8-11. G) Gene Ruler DNA Ladder mix in every first lanes.

3.3. AuNPs characterization

AuNPs were synthesized in the beginning of this work using sodium citrate as capping agent in order to achieve a final average diameter of 14 nm, as previously described in several reports in which non-crosslinking approaches were used (Costa *et al* 2010; Veigas *et al* 2010). To confirm if the desire size of AuNPs was obtained, the first simplest step was UV-vis spectroscopy analysis. The AuNPs presented a unique SPR absorbance peak in the region of 520 nm, more precisely

at 518 nm, confirming that the average diameter is approximately 14 nm, as expected (Huang *et al* 2007).

An alternative way to determine the AuNPs size was used, Dynamic light scattering (DLS). DLS is based on the differential scattering of the colloidal solutions conferred by their Brownian movement in the solution. The Brownian movement is related to the hydrodynamic radius of the AuNPs that differs with the molecules associated to its surface (Kato *et al*., 2009).

The results obtained through the DLS analysis showed that the AuNPs has an average diameter of 21.37 nm (±0.35), considerably higher than the predicted value of 14 nm. A possible cause for this discrepancy is the citrate capping of AuNPs witch alters the hydrodynamic radius of the AuNPs for higher values. According to this, the DLS results confirmed that the AuNPs had approximately the diameter required.

Finally, Transmission electron microscopy (TEM) analysis was performed to further confirm the average diameter of the AuNPs. TEM is a technique that generate images allowing the visualization of the AuNPs core and shape, providing a definitive and confinable confirmation for the size of the AuNPs. A representative image obtained by TEM analysis can be seen in figure 3.3.

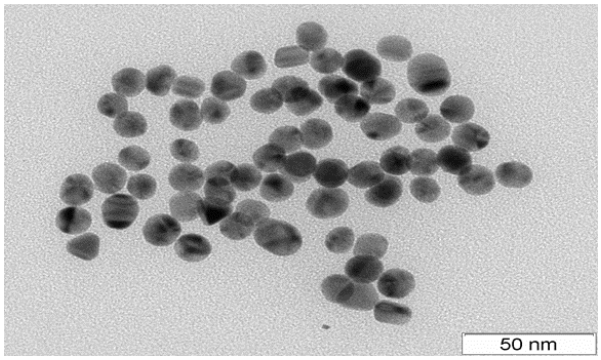

Figure 3.3 TEM image of spherical AuNPs with approximate 13 nm of diameter size.

AuNPs were counted and their size was measured to a total of 420 measurements. The calculated average diameter of the nanoparticles was 13.4 nm (±1.3), presented as a histogram to better visualize the size distribution (figure 3.4).

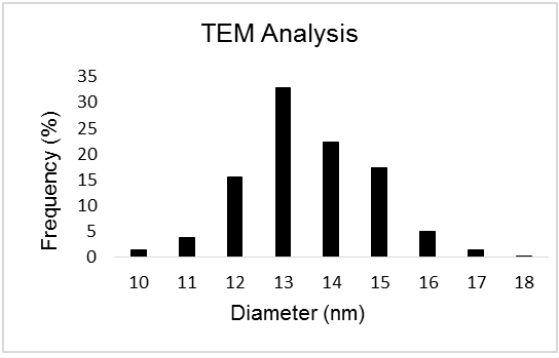

Figure 3.4 Histogram of the spherical AuNPs diameter analyzed by TEM.

3.4. Au-nanoprobes characterization

Once the desire size and shape of the AuNPs was confirmed, the next step was to functionalize the nanoparticles with the two probe sequences, mecA and mecA_V2 by salt-aging method (functionalize one amount of AuNPs with mecA probe and another amount of AuNPs with mecA_V2 probe). The functionalization was achieved by substituting the citrate ions on the surface of the AuNPs for thiol-modified oligonucleotides. The successive addition of salt, increasing the ionic strength resulted in the decrease of the electrostatic repulsion between the nanoparticles and allowed for the substitution of citrate ions for thiol groups.

As for the confirmation of the size of the AuNPs, the functionalization had to be confirmed prior to any subsequent assays with the Au-nanoprobes.

As before, the fastest and easiest way to verify the functionalization of the nanoparticles is to determine the UV-vis spectra. A successful functionalization will result in a shift of the maximum absorbance peaks to higher wavelengths. Both probes presented a shift in the SPR absorbance peak from 518 nm to 523 nm, indicating that the hydrodynamic radiuses of the nanoparticles had increased (figure 3.5).

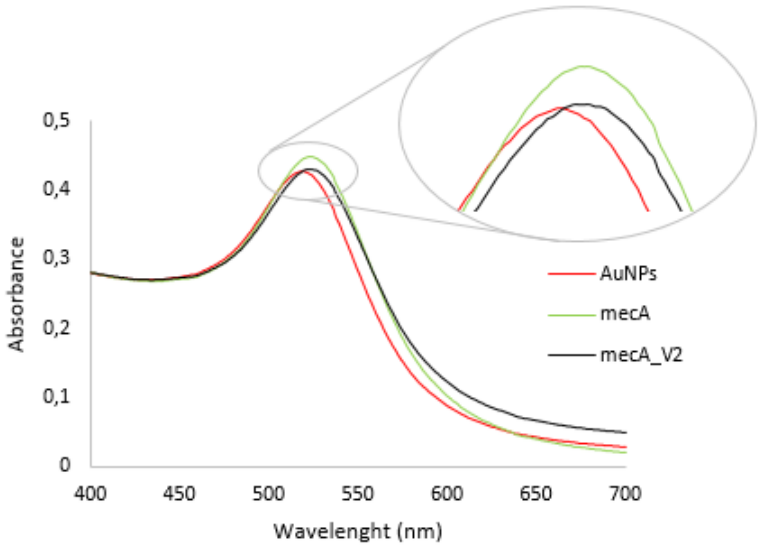

Figure 3.5 Spectra corresponding to AuNPs, mecA probe and mecA_V2 probe. The spectra was obtained by UV-Vis spectroscopy in the wavelength range of 400 - 700 nm.

To confirm this, the probes were analyzed by DLS. An increase in the hydrodynamic radius from 21.37 nm (±0.35) to 31.83 nm (±0.61) was observed for mecA probe and an increase to 32.93 nm (±0.40) was observed for mecA_V2 probe. The functionalization of AuNPs with an average diameter of 14 nm with 20 nucleotides probes is expect to yield Au-nanoprobes with 27.6 nm of diameter, since, according to Watson and Crick, the 20 nucleotides will cause an increase of 13.6 nm in the diameter of the nanoparticles (Watson and Crick, 1953). However, mecA probe only increased 10.46 nm the nanoparticle's diameter, while mecA_V2 probe increased 11.56 nm. These differences between the obtained and the expected results can be explained by the position of the oligonucleotides sequences that could be more "wavy" instead of being more

stretched. This could also meaning that the surface of the AuNPs has not the sufficient thiol-modified oligonucleotides attached, once with the electrostatic repulsion between the oligonucleotides sequences, the thiol-modified oligonucleotides should be stretched.

Stability assays were performed in order to evaluate the differences in the stability of the AuNPs colloid solution, once the citrate capped AuNPs aggregate by the increase of the ionic strength of the solution. As the oligonucleotides protect AuNPs from aggregation, by maintaining their stability in solution upon salt addition, it was expected that the Au-nanoprobes present the same stability when higher concentrations of salt were induced (Sato *et al*., 2003).

The stability assays for the Au-nanoprobes showed that the maximum shift in the SPR peak was to 594 nm for both probes. Also, the minimum concentrations of $MgCl_2$ needed to induce full aggregation of the Au-nanoprobes were determined as 65 mM for mecA_V2 probe and 110 mM for mecA probe, as shown in figure 3.6.

The value of the maximum shift in SPR peak for aggregated Au-nanoprobes and the value of SPR peak for dispersed Au-nanoprobes were used to define a reference ratio. Varied sets of wavelengths was studied in order to use the trapezoidal rule and to attain the highest numeric difference between dispersed and aggregated Au-nanoprobes. The intervals chosen was 10 nm before and after the SPR peaks for the dispersed and aggregated Au-nanoprobes, respectively. This ratio was used for all non-crosslinking assays and was set to define if there is more dispersed or aggregated Au-nanoparticles in solution. For ratio values lower than 1, nanoparticles were considered fully aggregated.

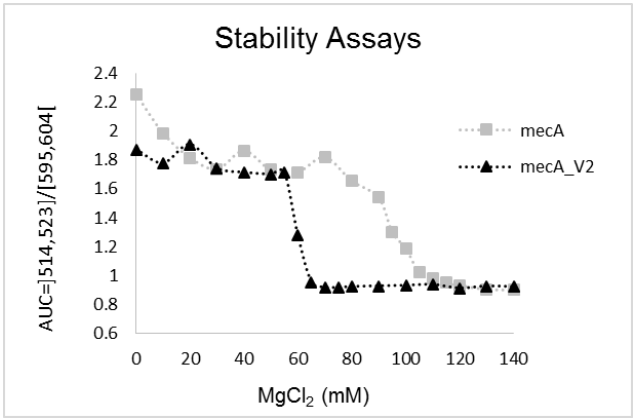

Figure 3.6 Au-nanoprobes stability assays using increasing concentrations of $MgCl_2$. AUC ratio was calculated and for values lower than 1, Au-nanoprobes were considered aggregated. 65 and 110 mM of $MgCl_2$ were considered the minimum concentrations needed to induce aggregation for mecA_V2 probe and mecA probe, respectively. The assays were all performed in triplicates.

3.5. Au-nanoprobes calibration

Once the functionalization of AuNPs was confirmed, it was necessary to verify if they were able to detect complementary targets and discriminate them from non-complementary targets. Therefore, synthetic oligonucleotides were used because they are single stranded and present a high purity level. As expected for the hybridization with a complementary target, the Au-nanoprobes showed an increase in stability, as observed in figure 3.7. The synthetic

oligonucleotides hybridize with the Au-nanoprobes forming double stranded DNA sequences that are more complex and stable than single stranded molecules (Li and Rothberg, 2004). These structures will improve the steric hindrance around AuNPs, increasing their stability in solution, preventing aggregation. Both probes were able of detect complementary targets and discriminate them from non-complementary targets.

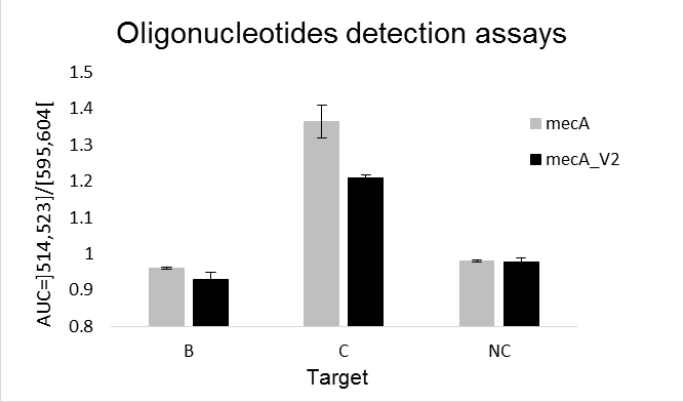

Figure 3.7 Au-nanoprobes detection assays using 3 pmol/µL of oligonucleotides. 110 mM of $MgCl_2$ was used in assays for mecA probe and 65 mM of $MgCl_2$ was used in assays for mecA_V2 probe. In B (Blank) assay, no DNA was added. In C assay, complementary target was added and in NC assay, non-complementary target was added. The assays were all performed in triplicates.

3.6. Detection of PCR products

Both probes were shown to be able of detect complementary targets using synthetic oligonucleotides. The next step was to determine if they were able to discriminate between complementary and non-complementary targets in the presence of higher DNA fragments sequences, double stranded and with several contaminants. Many components of the PCR reaction can interfere with Au-nanoprobes stability, such as dNTPs, proteins and salts (Eichmann and Bevan, 2010; Zhao *et al*., 2007). In order to remove the majority of these interfering compounds, the PCR products were purified by ethanol precipitation. Non-crosslinking colorimetric assays were performed using various concentrations of PCR products and the obtained results are shown in figure 3.8.

As expected, the results showed a direct correlation between the target concentration and the stability of the AuNPs, since higher concentrations of target mean higher stability of the AuNPs. The mecA_V2 probe seemed more sensitive and specific than mecA probe, as it presented higher ratios for the assays with the same concentrations of PCR products with the complementary target.

Although it was not possible to achieve a positive result for the detection of 10 ng/µL of target, we can see for both probes a slight discrimination between complementary target and non-complementary target.

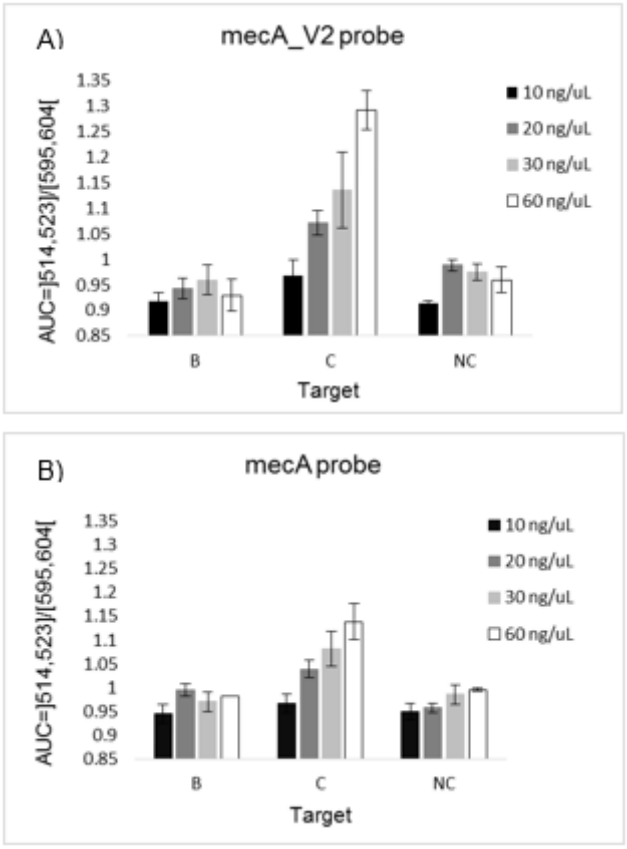

Figure 3.8 Au-nanoprobes detection assays using various concentrations of PCR product. 110 mM of $MgCl_2$ was used in A) mecA probe and 65 mM of $MgCl_2$ was used in B) mecA_V2 probe. In B (Blank) assay no DNA was added. In C assay, complementary target was added and in NC assay, non-complementary target was added. The targets were purified by ethanol precipitation. The assays were all performed in triplicates.

To improve the discrimination efficiency between the complementary target and the non-complementary, another purification method of the PCR products was tested: the PCR products were dialyzed using a membrane with MWCO of 3500 Da. All the assays were performed with mecA_V2 probe and the results are shown in figure 3.9.

A significant difference was observed in the stability of the Au-nanoprobes, after hybridization with a complementary target. The detection of the PCR products purified by dialysis showed an increase in AUC ratio for all the concentrations of PCR product, meaning that this purification method is more efficient than ethanol precipitation. With this method, a positive result was achieved for the concentration of 10 ng/µL of PCR product. One possible explanation is that the dialysis method removes more contaminants from the PCR reactions than ethanol precipitation. However, the yield of the dialysis method was lower than for ethanol precipitation. In the end, a choice has to be made between the yield and the purity level of the PCR product.

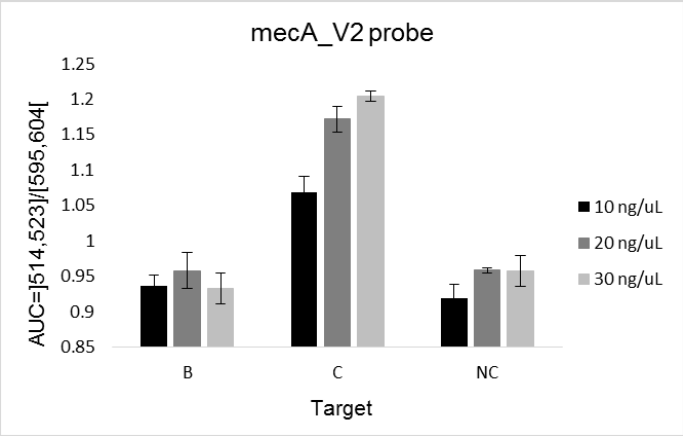

Figure 3.9 Au-nanoprobes detection assays using mecA_V2 probe and various concentrations of PCR product. 65 mM of $MgCl_2$ was used in all assays. In B (Blank) no DNA was added. In C assay, complementary target was added and in NC assay, non-complementary target was added. The targets were purified by dialysis. The assays were all performed in triplicates.

3.7. Detection of plasmid DNA

After the successful detection of the PCR products, the method was adapted for the detection of pDNA. By avoiding the amplification step, the time needed to obtain a final result as well as the associated costs, are decreased. Several studies showed impressive results using sonicated gDNA for application in biosensors, as fragmentation decreases the steric hindrance between the probes and the targets (Mann and Krull, 2004). The use of ultrasounds results in the fragmentation of biological molecules (Miller *et al*., 1996). The high frequency acoustic waves result in cavitation, the formation of microbubbles with gas. Inside this bubbles, high pressure and temperatures lead to mechanical and thermal degradation (Suslick *et al*., 1999).

Au-nanoprobes detection assays were performed with pDNA before and after fragmentation. Neither condition showed positive results, as presented in figure 3.10, indicating that fragmentation was not efficient for the detection of pDNA. For both probes the ratios were bellow 1, meaning that the Au-nanoprobes were not stable and consequently aggregated. A possible explanation would be the presence of contaminants or insufficient concentration of target needed for detection. In fact, pDNA consists on much longer DNA molecules than the PCR products. In this way, the same concentration of pDNA and PCR product corresponds to a much lower number of DNA fragments in the pDNA solution. Moreover, for high concentrations of target, the colorimetric assays cease to be economic and sensible.

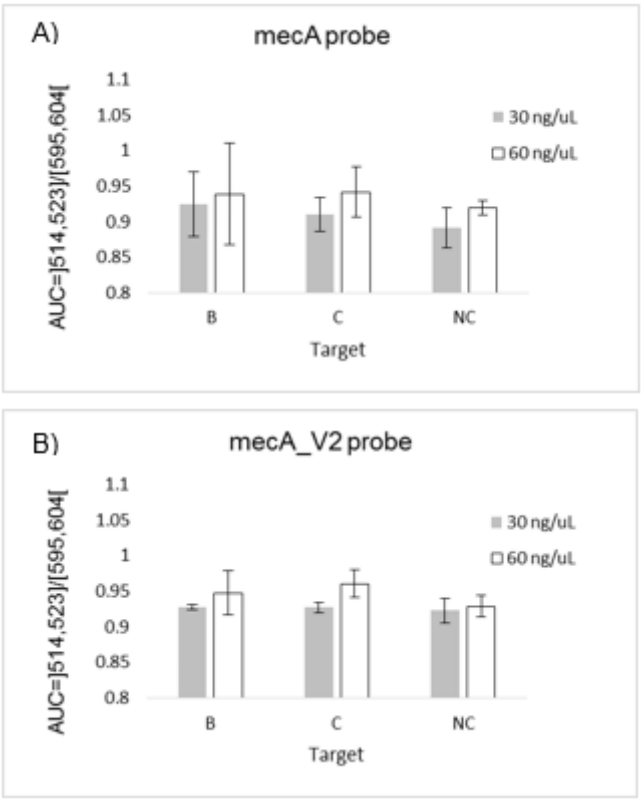

Figure 3.10 Au-nanoprobes detection assays using 30 and 60 ng/µL of sonicated pDNA. 110 mM of $MgCl_2$ was used in A) mecA probe and 65 mM of $MgCl_2$ was used in B) mecA_V2 probe. In B (Blank) assay no DNA was added. In C assay, complementary target was added and in NC assay, non-complementary target was added. The assays were all performed in triplicates.

3.8. Detection of genomic DNA

Although the detection with pDNA did not retrieve positive results, and in order to develop a faster and less costly diagnostic test, another target molecule that does not involve an amplification step was used: gDNA. In a first approach, Au-nanoprobes assays were performed with intact gDNA. All the tests showed positive results either for complementary targets as for non-complementary targets, showing no discrimination between them. This can be explain by the higher complexity and density of gDNA which may cause a buffer effect around the Au-nanoprobes preventing them to aggregate upon absurd concentration of salts. It was verified that for the maximum concentration of $MgCl_2$ used (500 mM) the increase of the ionic strength of the solution was not able to induce aggregation.

In order to produce smallest DNA fragments and some single stranded molecules gDNA fragmentation was performed (Mann and Krull, 2004), to achieve a better result in the biosensor test. The ultrasonic-based method proved to be efficient for the DNA fragmentation, as expected (Larguinho, *et al*., 2010). A significant difference between the complementary and non-complementary targets was observed for both probes. MecA probe seems to be more sensible than mecA_V2 probe as it was able to detect at the lowest target concentration (10 ng/µL). However, this discriminative capacity was lost for the target concentration of 30 ng/µL. The increase in target concentration increased the buffer effect of the target and decreased the efficiency of the system. On the other hand, mecA_V2 probe seems to be more specific; although

it was only able to detect at the target concentration of 20 ng/µL, the discrimination between complementary and non-complementary targets was maintained for all the target concentrations. In conclusion, both probes show the capacity to discriminate complementary from non-complementary targets. These results are shown in figure 3.11.

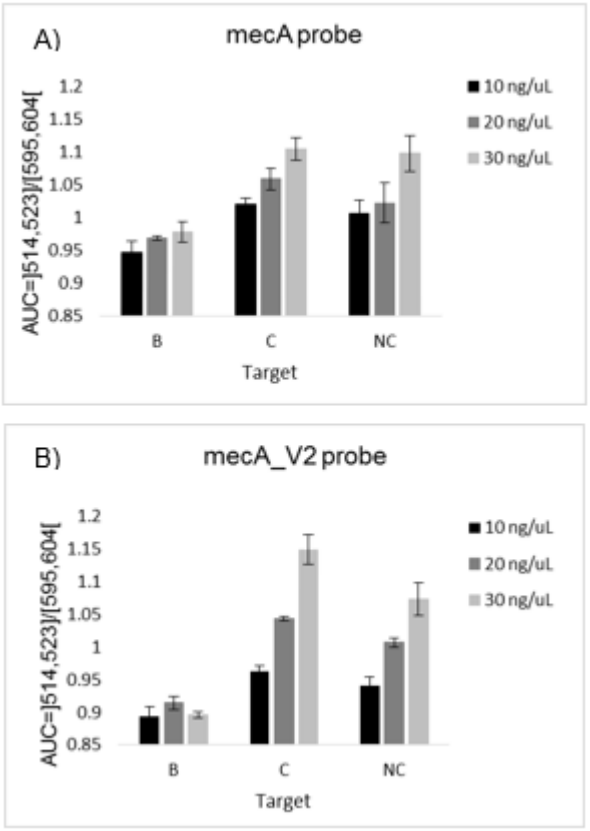

Figure 3.11 Au-nanoprobes detection assays using various concentrations of sonicated gDNA. 110 mM of $MgCl_2$ was used in A) mecA probe and 65 mM of $MgCl_2$ was used in B) mecA_V2 probe. In B (Blank) no DNA was added. In C assay, complementary target was added and in NC assay, non-complementay target was added. The assays were all performed in triplicates.

3.9. Detection of RNA

As gDNA detection was achieved with mecA and mecA_V2 probes the next step was to detect RNA. As RNA is single stranded and the two probes chosen for this work are sense and antisense, only one of them could be used for RNA detection. The probe with complementarity for the RNA sequence is the mecA_V2 probe.

NCL detection assays were performed using various concentrations of RNA and the results are presented in figure 3.12. No positive results were observed nor discrimination between complementary and non-complementary targets for all the concentrations tested. This can be due to many reasons: presence of contaminants in the target samples; denaturation of RNA or formation of secondary structures; insufficient target concentration.

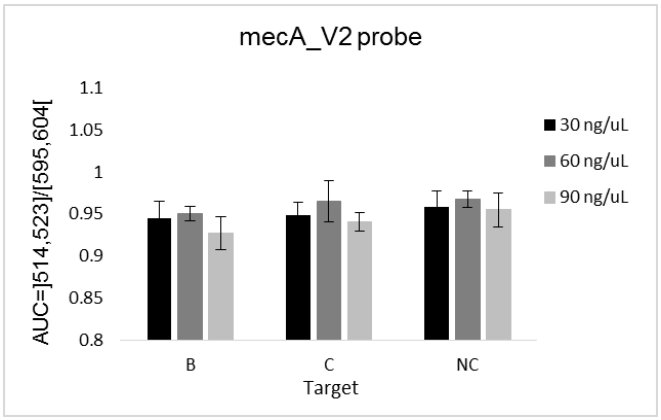

Figure 3.12 Au-nanoprobes detection assays using various concentrations of RNA. 65 mM of $MgCl_2$ was used in every assays. In B (Blank) assay no RNA was added. In C assay, complementary target was added and in NC assay, non-complementary target was added. The assays were all performed in triplicates.

Although the results for the RNA detection were negative, a spike-in approach was performed in order to verify if the Au-nanoprobes are able to detect complementary single stranded synthetic oligonucleotides in the presence of non-complementary RNA sequences that are much longer and evaluate if non-complementary sequences of RNA could interfere with detection.

Au-nanoprobes detection assays were performed using mecA_V2 probe. Various concentrations of non-complementary RNA were mixed with a fixed concentration of synthetic oligonucleotides complementary and non-complementary to mecA_V2 probe. The results are presented in figure 3.13. The ratio value seems to be affected by the increase in RNA concentration, for concentrations higher than 90 ng/µL. Not only the ratio value for the complementary target decreases, but also the ratio value for non-complementary increases for values above 1, meaning less discriminative efficiency and consequently less detection efficiency. The high concentration of RNA may result in the buffer effect of the nucleic acid as in gDNA assays.

Still, the developed system allows the detection and discrimination of single stranded nucleic acid sequences even in the presence of non-complementary sequences to a concentration of 90ng/µL.

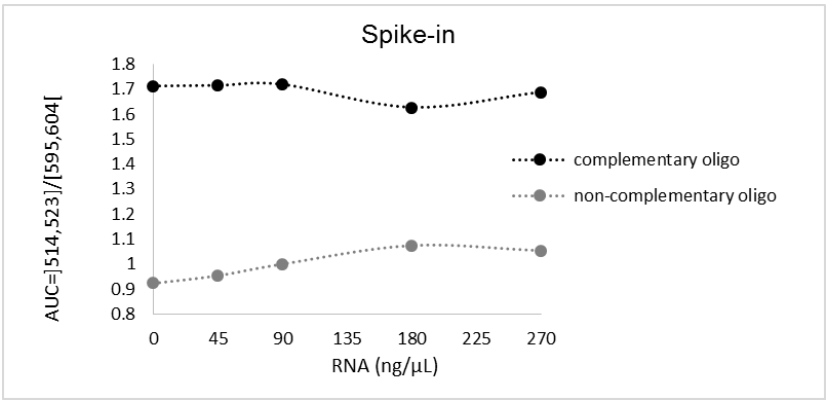

Figure 3.13 Au-nanoprobes detection assays using various concentrations of non-complementary RNA. 65 mM of $MgCl_2$ were added in every assay. The black curve represents the results for the assays with the fixed concentration of 10 pmol of complementary oligonucleotides. The grey curve represents the results for the assays with the fixed concentration of 10 pmol of non-complementary oligonucleotides. The assays were all performed in triplicates.

4. Conclusions and future perspectives

In this thesis it was intended the development of an Au-nanoprobes system based on non-crosslinking method in the detection of MRSA infections. With this propose, AuNPs were synthesized and functionalized with thiol-modified oligonucleotides. The desire size of the AuNPs was confirmed by TEM analysis and the hydrodynamic radius was measured by DLS, indicating the functionalization of the AuNPs.

The minimum $MgCl_2$ concentration required to induce full aggregation of the two Au-nanoprobes, mecA and mecA_V2, was defined at 110 mM and 65 mM, respectively.

Although the results of *mecA* gene detection in pDNA and RNA samples were negative, both probes presented ability to discriminate between complementary and non-complementary targets in PCR products and gDNA samples for target concentrations of 10 ng/µL and 20 ng/µL, respectively.

The purification of PCR products by dialysis showed lower yield values compared to ethanol precipitation but on the other hand it showed an increase in detection efficiency.

The developed Au-nanoprobes system with gDNA samples proved to be the best strategy to identify a MRSA infection, overcoming the actual techniques for diagnosis in time-consuming and costs, being also performed without the need of expensive and complex laboratory set up. With this system, after the gDNA extraction it is only takes 50 minutes to achieve a colorimetric result and an efficient detection of the presence of *mecA* gene. As gDNA can be extracted directly from blood samples and the procedure can be concluded in a day, the detection of MRSA infection would be possible within a day.

However, the efficiency of this method must be confirmed with clinical samples. Also, the cellular viability of the microorganisms should be measured. Also, optimizations must be done in order to improve the hybridization efficiency in the non-crosslinking colorimetric assays with RNA samples. This optimizations may provide a more even faster diagnostic, once the RNA extraction is faster than DNA extraction.

References

Acikgoz, C., Hempenius, M.A., Huskens, J., *et al*. 2011. Polymers in conventional and alternative lithography for the fabrication of nanostructures. Eur Polym. 47 2033-52

Archer, G.L., Pennell, E. 1990. Detection of methicillin resistance in staphylococci by using a DNA probe. Antimicrob Agents Chemother. 34:1720-4.

Bannerman, T.L. 2003. Staphylococci, Micrococcus and other catalase-positive cocci that grow aerobically. In: Murray, P.R., Baron, E.J., Jorgensen, J.M., *et al*. eds. Clin Microbiol. 384-404.

Baptista, P., Doria, G., Henriques, D., *et al*. 2005. Colorimetric detection of eukaryotic gene expression with DNA-derivatized gold nanoparticles. Biotechnology. 119:111-17.

Baptista, P.V., Koziol-Montewka, M., Paluch-Oles, J., *et al*. 2006. Gold-nanoparticle-probe-based assay for rapid and direct detection of Mycobacterium Tuberculosis DNA in clinical samples. Clin Chem. 52:1433-4.

Barakat, N. S. 2009. Magnetically modulated nanosystems: a unique drug-delivery platform. Nanomedicine. 4:799-812.

Barry, A.L., Lachica, R.V., Atchinson, F.W. 1973. Identification of *Staphylococcus aureus* by simultaneous use of tube coagulase and thermonuclease tests. Appl Microbiol. 25:496-7.

Brown, D.F., Walpole, E. 2001. Evaluation of the Mastalex agglutination test for methicillin resistance in *Staphylococcus aureus* grown on different screening media. Antimicrob Chemother. 47:187-9.

Chain, E., Florey, H., Gardner, A., Heatley, N., Jennings, M, *et al*. 1940. Symptoms relating. Lancet. 226-228.

Conde, J., de la Fuente, J.M., Baptista, P.V. 2010. RNA quantification using gold nanoprobes – application to cancer diagnostics. Nanobiotechnology. 8:5.

Conde, J., Dias, J.T., Grazú, V., Moros, M., Baptista, P.V., de la Fuente, J.M. 2014. Revisiting 30 years of biofunctionalization and surfasse chemistry of inorganic nanoparticles for nanomedicine. Front Chem. 2:48.

Cookson, B. 1997. *Staphylococcus aureus*. Princ Clin Bacteriol. 109-30.

Costa, P., Amaro, A., Botelho, A., Inacio, J., Baptista, P.V. 2010. Gold nanoprobe assay for the identification of mycobacteria of the Mycobacterium tuberculosis complex. Clin Microbiol Infect Dis. 16:1464-1469.

Couto, I., de Lencastre, H., Severina, E., Kloos, W., Webster, J.A., Hubner, R.J., Sanches, I.S., Tomasz, A. 1996. Ubiquitous presence of a *mecA* homologue in natural isolates of *Staphylococcus sciuri*. Microb Drug Resist. 2:377-391.

Crisostomo, M.I., Westh, H., Tomasz, A., Chung, M., Oliveira, D.C., de Lencastre, H. 2001. The evolution of methicillin resistance in *Staphylococcus aureus*: similarity of genetic backgrounds in historically early methicillin-susceptible and –resistant isolates and comtemporary epidemic clones. Proc Natl Acad Sci. 98:9865-70.

Dabul, A.N., Camargo, I.L. 2014. Molecular characterization of methicillin-resistant *Staphylococcus aureus* resistant to tigecycline and daptomycin isolated in a hospital in Brazil. Epidemiol Infect. 142: 479-83.

de Lencastre, H., Oliveira, D., Tomasz, A. 2007a. Antibiotic resistant *Staphylococcus aureus*: a paradigm of adaptive power. Curr Opin Microbiol. 10(5): 428-35.

de Lencastre, H., Tomasz, A. 2007b. Multiple stages in the evolution of the methicillin resistant *Staphylococcus aureus*. Am Soc Microbiol. 28:333-46.

Debnath, B., Shashank, S., Niraj, S., Ankesh, K., Seung-Hwan, J. 2009. Nanotechnology, Big things from a Tiny World: a Review. Serv Sci Technol. 2(3):29-38.

Dinges, M.M., Orwin, P.M., Schlievert, P.M. 2000. Exotoxins of *Staphylococcus aureus*. Clin Microbiol. 13:16-34.

Dreaden, E.C., Alkilany, A.M., Huang, X., Murphy, C.J., El-Sayed, M. 2012. The golden age: gold nanoparticles for biomedicine. Chem Soc Rev. 41(7):2740–79.

Duguid, J.G., Bloomfield, V.A. 1995. Aggregation of melted DNA by divalent metal ion-mediated cross-linking. Biophysical. 69:2642-8.

Eichmann, S. L., Bevan, M. A. 2010. Direct Measurements of Protein-Stabilized Gold Nanoparticle Interactions. Langmuir. 26**:**14409-14413.

Eustis, S., El-Sayed, M.A. 2006. Why gold nanoparticles are more precious than pretty gold: noble metal surface plasmon resonance and its enhancement of the radiative and nonradiative properties of nanocrystals of different shapes. Chem Soc Rev. 35:209-217.

Fisher, J.F., Meroueh, S.O., Mobashery, S. 2005. Bacterial resistance to beta-lactam antibiotics: compelling opportunism, compelling opportunity. Chem Rev. 105(2): 395-424.

Fleming, A. 1929. On the antibacterial action of cultures of a penicillium, with special reference to their use in the isolation of B. influenzae. Exp Pathol. 10: 226-236.

Foster, T.J. 2005. Immune evasion by staphylococci. Nat Rev Microbiol. 3(12): 948-58.

Foster, T.J., Hook, M. 1998. Surface protein adhesions of *Staphylococcus aureus*. Trends Microbiol. 6:484-488.

Fuda, C.C., Fisher, J. F., Mobashery, S. 2005. Beta-lactam resistance in *Staphylococcus aureus*: the adaptive resistance of a plastic genome. Cell Mol Life Sci. 62:2617-2633.

Grundmann, H., Aires-de-Sousa, M., Boyce, J., Tiemersma, E. 2006. Emergence and resurgence of meticillin-resistant *Staphylococcus aureus* as a public-health threat. Lancet. 368(9538): 874-85.

Grzelczak, M., Vermant, J., Furst, E.M., *et al*. 2010. Directed self-assembly of nanoparticles. Am Chem Soc Nano. 4:3591-605

Gu, B., Kelesidis, T., Tsiodras, S., Hindler, J., Humphries, R.M. 2013. The emerging problem of linezolid-resistant *Staphylococcus*. Antimicrob Chemother. 68(1): 4-11.

Hiramatsu, K., Cui, L., Kuroda, M., Ito, T. 2001. The emergence and evolution of methicillin-resistant *Staphylococcus aureus*. Trends Microbiol. 9:486-93.

Hiramatsu, K., Ito, T., Tsubakishita, S., Sasaki, T., Takeuchi, F., Morimoto, Y., Katayama, Y., Matsuo, M., Kuwahara-Arai, K., Hishinuma, T., Baba, T. 2013. Genomic Basis for Methicillin Resistance in *Staplylococcus aureus*. Infect Chemother. 45(2):117-136.

Holzinger, M., Le Goff, A., Cosnier, S. 2014. Nanomaterials for biosensing applications: a review. Front Chem. 2:63.

Huang, M.B., Gay, T.E., Baker, C.N., *et al*. 1993. Two percent sodium chloride is required for susceptibility testing of staphylococci with oxacillin when using agar-based dilution methods. Clin Microbiol. 31:2683-8.

Huang, X., Jain, P.K., El-Sayed, I.H., El-Sayed, M.A. 2007. Gold nanoparticles: interesting optical properties and recent applications in cancer diagnostics and therapy. Nanomedicine 2:681-693.

Hurst, S.J., Lytton-Jean, A.K.R., Mirkin, C.A. 2006. Maximizing DNA Loading on a Range of Gold Nanoparticle Sizes. Anal Chem. 78:8313-18.

Hutter, E., Fendler, J.H. 2004. Exploitation of localized surface plasmon resonance. Adv Mater. 16:1685-706.

International Working Group on the Classification of Staphylococcal Cassette Chromosome Elements (IWG-SCC). 2009. Classification of staphylococcal cassette chromosome *mec* (SCC*mec*): guidelines for reporting novel SCC*mec* elements. Antimicrob Agents Chemother. 53:4961-7.

Ito, T., Katayama, Y., Asada, K., Mori, N., Tsutsumimoto, K., Tiensasitorn, C., Hiramatsu, K. 2001. Structural comparison of three types of staphylococcal cassette chromosome *mec* integrated in the chromosome in methicillin-resistant *Staphylococcus aureus*. Antimicrob Agents Chemother. 45:1323–1336.

Jevons, M.P. 1961. Celbenin-resistant staphylococci. Br Med J. 2:124-33.

Ji, X., Song, X., Li, J., Bai, Y., Yang, W., Peng, X. 2007. Size Control of Gold Nanocrystals in Citrate Reduction: The Third Role of Citrate. Am Chem Soc. 129:13939-13948.

Joshi, B.P., Wang, T.D. 2010. Exogenous molecular probes for targeted imaging in cancer: focus on multi-modal imaging. Cancers. 2(2):1251-1287.

Katayama, Y., Zhang, H.Z., Hong, D., Chambers, H.F. 2003. Jumping the barrier to beta-lactam resistance in Staphylococcus aureus. Bacteriology. 185:5465-5472.

Kato, H., Suzuki, M., Fujita, K., Horie, M., Endoh, S., Yoshida, Y., Iwahashi, H., Takahashi, K., Nakamura, A., Kinugasa, S. 2009. Reliable size determination of nanoparticles using dynamic light scattering method for in vitro toxicology assessment. Toxicol in Vitro. 23**:**927-934.

Kernodle, D.S. 2000. Mechanisms of resistance to β-lactam antibiotics in Gram-positive pathogens. V.A. Fischetti, R.P. Novick, J.J. Ferretti, D.A. Portnoy, J.I. Rood, editors. Am Soc Microbiol. 609-620.

Kumar, D., Meenan, B.J., Mutreja, I., *et al*. 2012. Controlling the size and size distribution of gold nanoparticles: a design of experiment study. Int Nanosci. 11:1250023.

Kuroda, M., Ohta, T., Uchiyama, I., Baba, T., Yuzawa, H., Kobayashi, I., Cui, L., Oguchi, A., Aoki, K., Nagai, Y., *et al*. 2001. Whole genome sequencing of methicillin-resistant *Staphylococcus aureus*. Lancet. 357:1225-1240.

Kuusela, P., Hilden, P., Savolainen, K., *et al*. 1994. Rapid detection of methicillin-resistant *Staphylococcus aureus* strains not identified by slide agglutination tests. Clin Microbiol. 32:143-47.

Larguinho, M., Baptista, P.V. 2012. Gold and silver nanoparticles for clinical diagnostics – From genomics to proteomics. Proteomics. 75:2811-23.

Larguinho, M., Santos, H.M., Doria, G., Scholz, H., Baptista, P.V., Capelo, J.L. 2010. Development of a fast and efficient ultrasonic-based strategy for DNA fragmentation. Talanta. 81:881-886.

Larguinho, M., Santos, S., Almeida, J., *et al*. 2014. DNA adduct identification using gold-aptamer nanoprobes. IET Nanobiotechnol. 9(2):95-101.

Lee, J.H. 2003. Methicillin (Oxacillin)-resistant *Staphylococcus aureus* strains isolated from major food animals and their potential transmission to humans. Appl Environ Microbiol 69(11):6489-94

Leroy, Q., Raoult, D. 2010. Review of microarray studies for host-intracellular pathogen interactions. Microbiol Meth. 81:81-95.

Li, H., Rothberg, L. 2004. Colorimetric detection of DNA sequences based on electrostatic interactions with unmodified gold nanoparticles. Proc Natl Acad Sci. 101**:**14036-14039.

Ligozzi, M., Bernini, C., Bonora, M.G., *et al*. 2002. Evaluation of the VITEK 2 system for identification and antimicrobial susceptibility testing of medically relevant Gram-positive cocci. Clin Microbiol. 40:1681-86.

Love, J.C., Estroff, L.A., Kriebel, J.K., Nuzzo, R.G., Whitesides, G.M. 2005. Self-Assembled Monolayers of Thiolates on Metals as a Form of Nanotechnology. Chem Rev. 105:1103-1170.

Mann, L.T., Krull, U.J. 2004. The application of ultrasound as a rapid method to provide DNA fragments suitable for detection by DNA biosensors. Biosens Bioelectron. 20:945-955.

Mafuné, F., Kohno, J., Takeda, Y., *et al*. 2001. Formation of gold nanoparticles by laser ablation in aqueous solution of surfactant. Phys Chem. 105:5114-20

Marradi, M., Martín-Lomas, M., Penadés, S. 2010. Glyconanoparticles: polyvalent tools to study carbohydrate-based interactions. Adv Carbohydr Chem Biochem. 64:211-90.

Medeiros, A.A. 1997. Evolution and Dessimination of β-lactamases Accelerated by Generations of β-Lactam Antibiotics. Clin Infect Dis. 24(Suppl 1):S19-45.

Miller, M.W., Miller, D.L., Brayman, A.A. 1996. A review of in vitro bioeffects of inertial ultrasonic cavitation from a mechanistic perspective. Ultrasound Med Biol. 22:1131-1154.

Mühlig, S., Rockstuhl, C. 2013. Multipole Analysis of Self-assembled metamaterials. In: Rockstuhl, C., Scharf, T. Editors Amorphous Nanophotonics. Springer. 89-117

Nakatomi, Y., Sugiyama, J.A. 1998. A rapid latex agglutination assay for the detection of penicillin-binding protein 2. Microbiol Immun. 42:739-43.

National Committee for Clinical Laboratory Standards. 2003. Methods for Dilution Antimicrobial Susceptibility Tests for Bacteria that Grow Aerobically: Approved Standard M7-A6. NCCLS Wayne PA.

Ogston, A. 1883. Micrococcus poisoning. Anat Physiol. 17: 24-58.

Oliveira, D.C., Milheirico, C., de Lencastre, H. 2006. Redefining a structural variant of staphylococcal cassette chromosome *mec*, SCC*mec* type VI. Antimicrob Agents Chemother. 50:3457–3459

Peacock, S.J., Lina, G., Etienne, J., *et al*. 1999. *Staphylococcus schleiferi* subsp. *schleiferi* expresses a fibronectin-binding protein. Clin Microbiol. 67:4272-5.

Perfézou, M., Turner, A., Merkoçi, A. 2012. Cancer detection using nanoparticle-based sensors. Chem Soc Rev. 41:2606-22.

Rammelkamp, C.H., Maxon, T. 1942. Resistance of *Staphylococcus aureus* to the action of penicillin. Proc Soc Exp Biol Med. 51:386-389.

Richards, R., Bönnemann, H. 2005. Synthetic Approaches to Metallic Nanomaterials. In: Kumar, C.S.S.R., Hormes, J., Leuschner, C., Editors Nanofabrication Towards Biomedical Applications: Techniques, Tools, Applications and Impact. WILEY-VCH Verlag GmbH & Co. KGaA, Weinheim, Germany. 2.

Rolinson, G.N., Stevens, S., Batchelor, F.R., Wood, J.C., and Berger-Bachi, E.B. 1960. Bacteriological studies on a new penicillin-BRL.1241. Lancet. 2:564-7

Rosenbach. 1884. Microorganisms of wound infections. Wiesbaden. Quoted by Fleming, A. in “A system of bacteriology”.1929. Med Res Counc. 2: 11-28.

Sato, K., Hosokawa, K., Maeda, M. 2003. Rapid aggregation of gold nanoparticles induced by non-crosslinking DNA hybridization. Am Chem Soc. 125:8102-8103.

Sato, K., Hosokawa, K., Maeda, M. 2005. Non-crosslinking gold nanoparticle aggregation as a detection method for single-base substitutions. Nucleic Acids Res. 33:e4.

Scheffers, D., Pinho, M.G. 2005. Bacterial Cell Wall Synthesis: New Insights from Localization Studies. Microbiol Mol Biol Rev. 69(4):585-607.

Shahmoon, A., Limon, O., Girshevitz, O., *et al*. 2010. Tunable nano devices fabricated by controlled deposition of gold nanoparticles via focused ion beam. Microelectron Eng. 87:1363-6

Shutter, J., Hatcher, V.B., Lowy, F.D. 1996. *Staphylococcus aureus* binding to human nasal mucin. Infect Immun. 64:310-8.

Singh, B. R., Singh, B. N., Khan, W., Singh, H. B., Naqvi, A. H. 2012. ROS-mediated apoptotic cell death in prostate cancer LNCaP cells induced by biosurfactant stabilized CdS quantum dots. Biomaterials 33:5753-5767.

Skaar, E.P., Schneewind, O. 2004. Iron-regulated surface determinants (isd) of *Staphylococcus aureus*: stealing iron from heme. Microbes Infect. 6:390-397.

Skinner, D., Keefer, C.S. 1941. Significance of bacteremia caused by *Staphylococcus aureus*. Intern Med. 68:851-875.

Solberg, C.O. 1965. A study of carriers of *Staphylococcus aureus* with special regard to quantitative bacterial estimations. Acta Med Scand Suppl. 436: 1-96.

Sperling, R.A., Parak, W.J. 2010. Surface modification, functionalization and bioconjugation of colloidal inorganic nanoparticles. Phil Trans R Soc A. 373:1333-83.

Sun, L., Zhang, Z., Wang, S., *et al*. 2009. Effect of pH on the interaction of gold nanoparticles with DNA and application in the detection of Human p53 gene mutation. Nanoscale Res Lett. 4:216-20.

Suslick, K.S., Didenko, Y., Fang, M.M., Hyeon, T., Kolbeck, K.J., McNamara III, W.V., Mdeleni, M.M., Wong, M. 1999. Acoutic cavitation and its chemical consequences. Phil Trans R Soc A. 357:335-353.

Takano, T., Higuchi, W., Otsuka, T., Baranovich, T., Enany, S., Saito, K., Isobe, H., Dohmae, S., Ozaki, K., Takano, M., Iwao, Y., Shibuya, M., Okubo, T., Yabe, S., Shi, D., Reva, I., Teng, L.J., Yamamoto, T. 2008. Novel characteristics of community-acquired methicillin-resistant *Staphylococcus aureus* belonging to multilocus sequence type 59 in Taiwan. Antimicrob Agents Chemother. 52:837–845

Thaxton, C., Georganopoulou, D., Mirkin, C. 2006. Gold nanoparticle probes for the detection of nucleic acid targets. Clin Chim Acta. 363:120-6.

Tipper, B.Y.D.J., Strominger, J.L. (1965). Mechanism of action of penicillins: a proposal based on their structural similarity to acyl-D-alanyl-D-alanine. Microbiology. 54:1163-1141.

Turkevich, J., Stevenson, P.C., Hillier, J. 1951. A study of the nucleation and growth processes in the synthesis of colloidal gold. Discuss Faraday Soc. 11:55-75.

van Bambeke, F., Lambert, D.M., Mingeot-Leclercq, M.P., Tulkens, P.M. 2003. Anti-infective therapy: Mechanism of action. Infect Dis. 7.1.1-7.1.14.

Vandenesch, F., Naimi, T., Enright, M.C., Lina, G., Nimmo, G.R., Heffernan, H., Liassine, N., Bes, M., Greenland, T., Reverdy, M.E., Etienne, J. 2003. Community-acquired methicillin-resistant *Staphylococcus aureus* carrying Panton-Valentine leukocidin genes: worldwide emergence. Emerg Infect Dis. 9:978–984.

Vanderbergh, M.F.Q., Verbrugh, H. A. 1996. From the chicago meetings. 525-534.

Veigas, B., Machado, D., Perdigao, J., Portugal, I., Couto, I., Viveiros, M., Baptista, P. V. 2010. Au-nanoprobes for detection of SNPs associated with antibiotic resistance in Mycobacterium tuberculosis. Nanotechnology. 21**:**415101.

Watson, J. D., Crick, F. H. 1953. Molecular structure of nucleic acids; a structure for deoxyribose nucleic acid. Nature. 171**:**737-738.

Wichelhaus, T.A., Kern, S., Schafer, V., *et al*. 1999. Evaluation of modern agglutination tests for identification of methicillin-susceptible and methicillin-resistant *Staphylococcus aureus*. Clin Microbiol Infect Dis. 18:756-8.

Yocum, R.R., Waxman, D.J., Rasmussent, J.R., Stromincser, J.L. 1979. Mechanism of penicillin action: Penicillin and substrate bind covalently to the same active site serine in two bacterial D-alanine carboxypeptidases. Biochemistry. 76(6): 2730-2734.

Zhao, W., Lee, T. M. H., Leung, S. S. Y., Hsing, I. M. 2007. Tunable Stabilization of Gold Nanoparticles in Aqueous Solutions by Mononucleotides. Langmuir 23**:**7143-7147.

Appendix

A1 - Results of the DNA sequencing analysis plus primers.

mecA gene amplification sequence

GAACAGCATATGAGATAGGCATCGTTCCAAAGAATGTATCTAAAAAAGATTATAAAGCAATC
GCTAAAGAACTAAGTATTTCTGAAGACTATATCAAACAACAAATGGATCAAAATTGGGTACA
AGATGATACCTTCGTTCCACTTAAAACCGTTAAAAAAATGGATGAATATTTAAGTGATTTCG
CAAAAAAATTTCATCTTACAACTAATGAAACAGAAAGTCGTAACTATCCTCTAGGAAAAGCG
ACTTCACATCTATTAGGTTATGTTGGTCCCATTAACTCTGAAGAATTAAAACAAAAAGAATAT
AAAGGCTATAAAGATGATGCAGT

P. falciparum amplification sequence

CAGATGTCAGAGGTGAAATTCTAAGATTTTCTGGAGACGGACTACTGCGAAAGCATTTGCC
TAATCTATTTCCATTAATCAAGAACGAAAGTTAAGGGAGTGAAGACGATCAGATACCGTCGT
AATCTTAACCATAAACTATACCGACTAGGTGTTGGATGAATATAAAAAATATATAAATATGTA
GCATTTCTTAGGGAATGTTGATTTTATATTAGAATTGCTTCCTTCAGTACCTTATGAGAAATC
AAAGTCTTTGGGTTCTGGGGCGAGTATTCGCGCAAGCGAGAAAGTTAAAAGAATTGACGG
AAGGGCACCACCAGGCGTGGAGCTTGCGGCTTAATTTGACTCAACACGGGAAAACTCACT
AGTTTAAGACAAGAGTAGGATTGACAGATTAATAGCTCTTTCTTGATTTCTTGGATGGTGAT
GCATG